Aalto-yliopisto
Insinööritieteiden
korkeakoulu

Davide Conti

A techno-economic assessment for optimizing methanol production from woody biomass for maritime transport in Sweden

Diplomityö, joka on jätetty opinnäytteenä tarkastettavaksi diplomi-insinöörin tutkintoa varten.

Espoossa 15.08.2019
Examiner: Professor Annukka Santasalo-Aarnio
Supervisor: Annukka Santasalo-Aarnio
Supervisor: Fumi Maeda Harahap

Aalto University
School of Engineering

Aalto University, P.O. BOX 11000, 00076 AALTO
www.aalto.fi

Abstract of master's thesis

Author Davide Conti

Title of thesis A techno-economic assessment for optimizing methanol production from woody biomass for maritime transport in Sweden

Master programme Innovative and Sustainable Energy Engineering

Kirjoita tekstiä napsauttamalla tätä.

Thesis supervisor Annukka Santasalo-Aarnio

Thesis advisor(s) Annukka Santasalo-Aarnio, Fumi Maeda Harahap

Date dd.mm.yyyy **Number of pages** 73 **Language** English

Abstract

The maritime transport sector is currently highly dependent on oil-based fuels. International regulations enforce tight limits regarding NOx emissions from the exhaust gases and maximum sulphur content in the fuel, enhancing the sector interest towards the development of cleaner alternative fuels. A transition to biomass-based liquid fuels is of interest as a solution for reducing pollutant emissions and for CO2 emissions mitigation. This thesis investigates the techno-economic and environmental impacts of methanol production from solid wood residues in maritime transport of Sweden. Methanol seems to be a promising alternative to heavy and light fossil oils as maritime fuel, and sawmills residues are an abundant resource in Sweden. The study considers the entire methanol production chain, from assessing the availability of sawmill by-products until delivering the methanol to the Swedish ports. The analysis considers two methanol blending scenarios until year 2035, i.e., M5 and M25. Four possible plant sizes are considered, 100, 200, 300 and 400 MW of biomass fuel thermal input. The production plant is modelled in Aspen Plus to determine the material and energy streams involved in the process and to obtain the cost and efficiency of producing methanol at the synthesis plant. An optimization model developed in GAMS is used to locate the methanol production plants, so to minimize the cost of the production chain. The results include the final methanol cost and an estimation of the CO_2 emissions reduction potential from replacing oil fuels with methanol for the assumed scenarios.

Keywords Gasification, Maritime Transport, Methanol, Sweden, Woody Biomass.

Table of contents

Cover page
Abstract
Nomenclature
Abbreviation
Table of contents 2
Nomenclature 3
Abbreviations 5
1 Introduction 6
1.1 Scope, research objectives and methods 9
1.2 Literature review and research gap 10
1.3 Thesis structure 11
2 Emission standards regulation for marine transport and marine fuels 12
3 Biomass to methanol fuel conversion 14
3.1 Methanol production 14
3.1.1 Methanol from woody biomass 15
3.2 Methanol use as fuel 21
4 Data and methods for modelling the methanol synthesis plant 24
4.1 Gasification unit 24
4.2 Syngas upgrade 26
4.3 Methanol synthesis 28
5 Optimization model for defining methanol plant locations 29
5.1 Biomass supply 29
5.2 Costs of methanol production plant 32
5.3 Marine transport fuel demand 33
5.4 Optimization model 35
5.5 Summary of model assumptions 38
6 Method for estimating the GHG emission reduction potential 40
7 Scenario development 41
8 Results and discussions 42
8.1 Methanol plant's model results 42
8.2 Optimal methanol plant's sizes and locations 43
8.3 Total cost 46
8.4 GHG emissions reduction potential 46
8.5 Sensitivity analysis on maximum methanol transport distance 47
8.6 Sensitivity analysis on plant biomass-to-methanol conversion efficiency 49
9 Conclusions 52
References 54
Appendix 1 1
Appendix 2 4
Appendix 3 6
Appendix 4 10
Appendix 5 12
Appendix 6 14

Table of figures

Figure 1-1 *Transport final energy demand for OECD and non-OECD countries in PBtu (1 PBtu = 293.1 TWh) [5]* 6
Figure 1-2 *EU CO_2 emissions per sector from 1990 to 2014 (source EEA) [9]* 7
Figure 1-3 *Domestic transport: fuel energy use in 2016 in TWh (left) and use of biofuels from 1995 to 2016 in TWh (right) [14]* 8
Figure 3-1 *Global methanol demand in 2015 by end-use (left) and by region (right) [30]* 14
Figure 3-2 *C-H-O ternary diagram[1] of gasification process with steam (S), hydrogen (H) and oxygen (O) [38]* 16
Figure 3-3 *Effect of the gasification temperature on the obtained products [39]* 18
Figure 3-4 *Atmospheric steam-blown indirect gasifier (left) and pressurized direct oxygen fired gasifier (right) (modified from [40])* 18
Figure 3-5 *Quench (a), adiabatic with indirect cooling (b) and isothermal (c) reactors for methanol synthesis [45]* 21
Figure 5-1 *Geographical position and classification per annual production capacity of Swedish sawmills* 29
Figure 5-2 *Material balance of typical Swedish sawmill ($\%_{weight,}$ dry) [61]* 30
Figure 5-3 *Historical prices for wood chips and sawdust in Sweden [13]* 31
Figure 5-4 *Final energy use for international (left axis) and domestic transport (right axis) in Sweden from 1976 [13]* 33
Figure 5-5 *Projected final demand for international marine transport* 34
Figure 5-6 *Geographic position of Swedish ports and classification per annual energy demand (in GWh)* 35
Figure 8-1 *Optimal locations of methanol production plants for scenarios M5 (left) and M25 (right)* 43
Figure 8-2 *Gross GHG emissions avoided (left axis) and resulting GHG emissions reduction in comparison to 2016 levels (right axis).* 47
Figure 8-3 *Variation of bio-methanol LCOE as function of the maximum imposed air distance between methanol producer and receiving port* 47
Figure 8-4 *Results of sensitivity analysis on the variation of distance's constraint for methanol transport in percentage compared to the base scenario.* 48
Figure 8-5 *Variation of bio-methanol LCOE as function of the ratio between the new assumed plant efficiency and the value considered in the base scenario* 49
Figure 8-6 *Results of sensitivity analysis on the variation of plant efficiency in percentage compared to the base scenario* 50

Appendix

Figure B-1 *Aspen Plus flowsheet simulation of the indirect gasification process* 4
Figure B-2 *Aspen Plus flowsheet simulation of the isothermal low-pressure methanol synthesis, with recirculation of unreacted gas and hydrogen* 4
Figure B-3 *Aspen Plus simulation of syngas cleaning and upgrade* 5
Figure E-1 *Bio-methanol plants individuated for different maximum methanol delivery distance imposed in M5 scenario* 12
Figure E-2 *Bio-methanol plants individuated for different maximum methanol delivery distance imposed in M25 scenario* 13
Figure F-1 *Bio-methanol plants individuated in M5 scenario for different assumed plant conversion efficiencies* 14
Figure F-2 *Bio-methanol plants individuated in M25 scenario for different assumed plant conversion efficiencies* 15

List of tables

Table 2-1 *MARPOL Annex VI NOx emission limits [27]* 12
Table 3-1 *Syngas contaminants requirements for methanol synthesis [41]* 18
Table 3-2 *Comparison of methanol and HFO fuel properties [50, 51]* 22
Table 4-1 *Ultimate and proximate analysis of biomass feedstock [56]* 24
Table 4-2 *Composition of product gas obtained after gasification [58]* 25
Table 4-3 *Description of blocks used for modelling biomass gasification* 26
Table 4-4 *Description of blocks included in the syngas upgrade model* 27
Table 4-5 *Description of blocks used for modelling the methanol synthesis process* 28
Table 5-1 *Scaling factors and cost of plant components referred to a 380 MW_{th} (LHV_{dry} biomass input) methanol synthesis plant [66, 67, 68]* 32
Table 5-2 *Other considered investment costs [66, 69]* 33
Table 5-3 *European market price for marine fuels used in the Baltic sea [74, 75, 76]* 38
Table 6-1 *Tank-to-propeller GHG emission factors for principal maritime fuels used in the Baltic sea [15]* 40
Table 8-1 *Obtained electric power consumption of bio-methanol synthesis plant* 42
Table 8-1 *Characteristics of methanol plants for M5 scenario* 44
Table 8-2 Characteristics of methanol plants for M25 scenario 44
Table 8-3 *Summary of costs for M5 and M25 base scenarios* 46
Table 8-5 *Results from efficiency sensitivity analysis on scenario M25: number of individuated bio-methanol plants and total installed biomass input capacity* 50
Appendix
Table A-1 *Design specification AIR-DRY* 1
Table A-2 *Design specification AIR-COMB* 1
Table A-3 *Design specification T-COMB* 1
Table A-4 *Design specification WAT-REF* 2
Table A-5 *Design specification WAT-WGS* 2
Table A-6 *Design specification BP-RATIO* 3
Table A-7 *Design specification GAS-REC* 3
Table A-8 *Design specification H2-REC* 3
Table C-1 *Position and production capacity of sawmills in Sweden (only sawmills with production capacity >30,000 m3/year)* 6
Table D-1 *Location of Swedish ports and loaded cargo for international and domestic shipping in 2016 [71]* 10

Nomenclature

CH_4 methane
C_2H_4 ethylene
C_2H_6 ethane
CO carbon monoxide
CO_2 carbon dioxide
HCl hydrogen chloride
H_2S hydrogen sulphide
NH_3 ammonia
NO_x nitrogen oxides
N_2O nitrous oxide
SO_x sulphur oxides

Abbreviations

CBB crop-based biofuels
CI compression ignition
DF dual fuel
EU European Union
ETS Emission Trading System
FAME Fatty Acid Methyl Esters
FO heavy fuel oil
GHG Greenhouse Gases
H_2/CO hydrogen-to-carbon ratio
HHV Higher Heating Value
HVO Hydrogenated Vegetable Oil
ICE internal combustion engine
IFO Intermediate Fuel Oil
LCOE Levelized Cost of Energy
LHV lower heating value
LNG Liquified Natural Gas
MeOH Methanol
MGO Marine Gasoil
MILP Mixed Integer Linear Programming
PM particulate matter
SN stoichiometric number
ULSFO ultra-low sulphur fuel oil
WGS water-gas-shift

1 Introduction

Reducing the environmental impact of the transport sector is one of the main challenges of our time. While the global energy demand for transport purposes is predicted to rise, as displayed in Figure 1-1, the dependency on fossil fuels must be reduced in order to lower the emission of Greenhouse Gases (GHG), as agreed within the Paris Agreement [1]. Compared to global electricity and heat generation, transport has the lowest penetration of renewable energy sources, which are mostly made up of biofuels for road transport [2]. In 2016, 93% of the global transport final energy use was dominated by fossil oil products [3] and the sector was the second largest source of CO_2 emissions, responsible for 24% of worldwide CO_2 emission level [4].

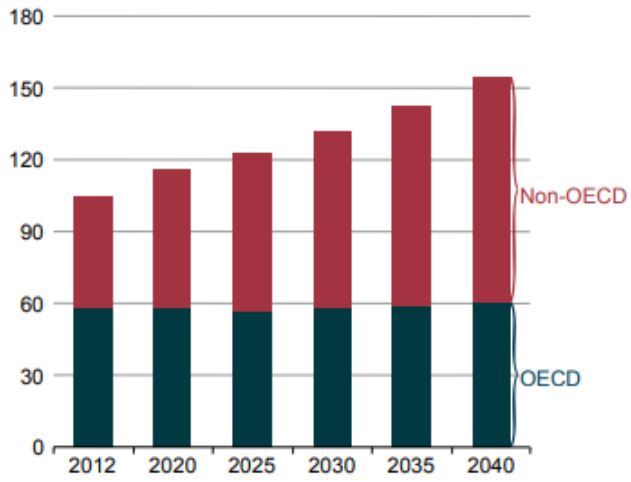

Figure 1-1 *Transport final energy demand for OECD and non-OECD countries in PBtu (1 PBtu = 293.1 TWh) [5]*

In the recent years, European Union (EU) and its member states governments have issued policies aiming to boost the penetration of renewable energy sources in the transport sector. At the EU level, on November 2016 the European Commission (EC) published a proposal to revise the Renewable Energy Directive (2009/28/EC), stating that the Member States must ensure that by 2020 at least 10% of their transportation fuels will come from renewable sources [6]. The share is increased to 14% of the total energy consumption by 2030 [6]. The policy also aims to reduce the use of crop-based biofuels (CBB) by limiting the share to 7% by 2020, the final goal is to decarbonize the transport sector and address the Indirect Land Use Change associated to food-based biofuels [6]. An average renewable share of 7.1%1 between all the EU member states was reached in 2016, with Sweden being one of the only two countries already reaching the target fixed for 2020 and registering a 30.3%[1] share of renewable energy used in transport [7].

Despite the legislation effort made by the EU, transport remains the highest CO_2 emitting sector in the EU and the only one that hasn't lowered its CO_2 emissions compared to the 1990 level. Figure 1-2 reports the historical variation of CO_2 emissions in the EU between 1990 and 2014. The EU identifies three priority areas for action to reduce emissions in transportation sector [8]:

- increasing the efficiency of the transport system by making the most of digital technologies, smart pricing and further encouraging the shift to lower emission transport modes;

[1] Calculations made according to Directive 2009/28/EC

- speeding up the deployment of low-emission alternative energy for transport, such as advanced biofuels, electricity, hydrogen and renewable synthetic fuels and removing obstacles to the electrification of transport;
- starting a transition towards zero-emission vehicles.

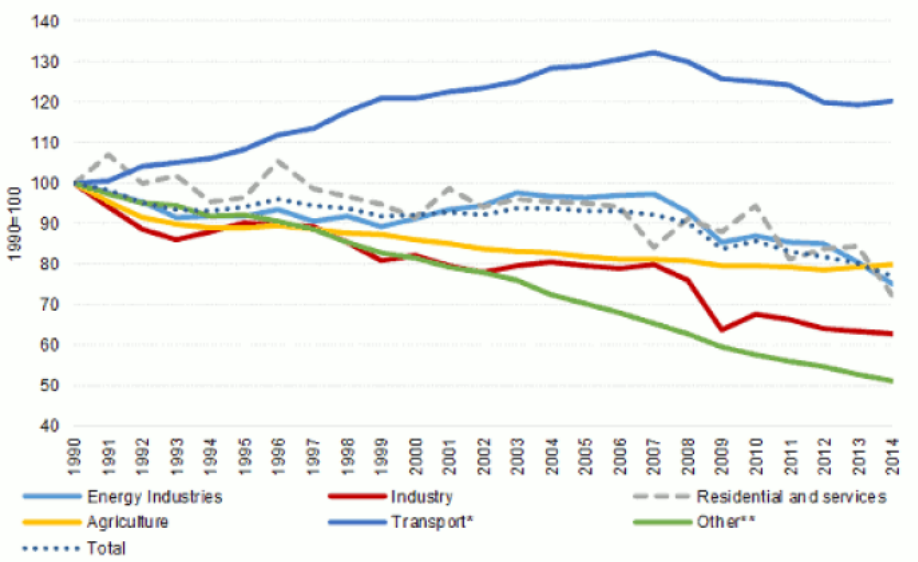

Figure 1-2 *EU CO_2 emissions per sector from 1990 to 2014 (source EEA) [9]*

Since the transport sector was not originally included in the EU Emission Trading System (ETS), EU's main tool to tackle GHG emissions and combat climate change, in May 2018 the European Parliament and the Council of the European Union approved the Effort Sharing legislation (EU regulation 2018/842) which defined GHG emission targets for those sectors not included in the ETS [10]. For non-ETS sectors, the legislation defines a GHG emissions reduction target of 30% by 2030 compared to 2005 levels [10]. The target should be delivered collectively by the member states of the EU, which were allocated with different final goals to ensure fairness between high income and low-income member states. Sweden was assigned a 40% GHG emission reduction target, the highest among the member states [11].

Nevertheless, the Swedish Parliament adopted in June 2017 a national climate policy (Govt. Bill 2016/17:146) which set the GHG emission reduction target for non-ETS to 63% by 2030 and an emissions reduction goal of 70% by the same year for domestic transport, compared to 2010 levels [12]. In 2016, the energy use for the transport sector in Sweden amounted to 121.1 TWh, of which 20% was dedicated to shipping, combining domestic and international marine transport [13]. Figure 1-3 shows that biofuels counted for 17% of the 2016 total energy consumption for domestic transport purposes [14].

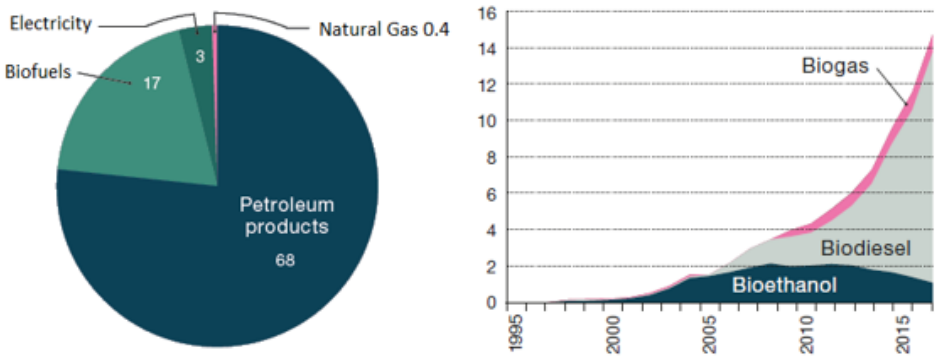

Figure 1-3 *Domestic transport: fuel energy use in 2016 in TWh (left) and use of biofuels from 1995 to 2016 in TWh (right) [14]*

The Swedish domestic use of biofuels, in particular biodiesel products, increased exponentially in the past 10 years (Figure 1-3 right), as response to the previously presented emission reduction targets and policies promoting renewable energy sources set by the EU. Fatty Acid Methyl Esters (FAME) and Hydrogenated Vegetable Oil (HVO) are the two main biodiesel products in the Swedish market [13]. While FAME biodiesels were mainly obtained from rapeseed oil, HVO used either slaughterhouse waste, crude tall oil or oil from vegetable and animal waste as feedstock [13]. Despite increased consumption of biofuels, the Swedish marine transport sector remains highly dependent on fossil-based fuels. In 2014, fuel oil (FO) products and marine gasoil (MGO) supplied all the energy consumed by the shipping industry, covering 80% and 20% of the demand respectively [15].

However, the raising concern regarding climate change and the new regulation about pollutant emissions enforced on marine transport applications, which is presented in section 2, are incentivizing a transition towards cleaner fuels. The regulation limits the emissions of Nitrogen oxides (NOx) from the exhaust gases and addresses the reduction of Sulphur oxides (SOx) emissions by enforcing a maximum allowed content of Sulphur in the fuel. Considering these requirements, methanol represents a valid alternative to the conventional petroleum derived fuels (i.e., FO, MGO and marine diesel oil (MDO)) that are currently used for maritime transport. In fact, NOx and particulate matter (PM) emissions from a compression ignition (CI) engine decline when a portion of the conventional fossil fuel is replaced by methanol, allowing greater emission reductions when the methanol fraction is increased [16]. Also, the absence of sulphur in the methanol directly eliminates the emissions of SOx. The combination of these effects can potentially eradicate the need of sophisticated systems for flue gas treatment, which are currently a necessity to comply with tightening pollutant emission standards when operating with conventional petroleum derived marine fuels.

The propulsion technology necessary for operating with methanol as marine fuels is considered mature, methanol can be used in dual fuel (DF) engines along with another conventional marine fuel or blended with FO for direct injection in a traditional compression ignition (CI) engine [17]. Furthermore, being a liquid fuel, the transport and handling of methanol does not introduce great challenges for what concerns the fuel transportation network, but existing fuel storage and distribution facilities must be adapted for the purpose of handling methanol [18].

Other than reducing NOx and SOx emissions, GHG emissions can also be decreased if the methanol used for replacing the conventional marine fuels is produced from a renewable

energy source, like biomass. This study considers the opportunity of producing bio-methanol, to use for marine transport purposes, from woodchips and sawdust that remains as by-products after the sawmilling process. Industrial sawmills are largely diffused in Sweden, where the forestry industry holds an important position in the national economy, providing 10% of the globally traded sawn timber, pulp and paper [19]. Given the considerable energy consumption for marine transport in Sweden, partially replacing the fossil-based marine fuels with bio-methanol can contribute to reduce the GHG emissions in the transport sector and at the same time decreasing the dependency of fossil fuels in the Swedish energy system.

1.1 Scope, research objectives and methods

The research aims at investigating the techno-economic impacts of methanol production from solid wood residues in maritime transport of Sweden. Furthermore, the study estimates the possible GHG emission reduction potential from replacing conventional marine fuels with bio-methanol, considering only the emissions related to the use of the fuel in the vessel by conducting a tank-to-propeller emission analysis. The methanol demand is expected to satisfy partly the domestic and international Swedish energy demand. More details concerning the estimation of the marine energy demand are reported in section 5.3.

The mainland boundaries of Sweden are set as the geographical boundaries of the model. The feedstocks considered are woodchips and sawdust, by-products generated by the sawmilling process. 116 sawmills positioned within these limits are considered as feedstock suppliers, all having a rated production capacity higher than 30000 m^3 of sawn wood per year. The availability of raw material is assessed by applying a material balance on the products obtained after the sawmilling process.

The study considers a planning horizon of 20 years starting from 2016, the last year with available data on Swedish maritime energy demand. An analysis of the historical data is performed to project the energy consumption over the timespan of the study. Then, the total energy demand is divided between the selected ports that are located inside the system boundaries.

The methanol plant is modelled with Aspen Plus. The model allows to quantify the material and energy streams involved in the conversion process. These are considered for estimating the plant's operation costs, which are included in the optimization model. The Aspen Plus model also provides the conversion efficiency of the plant, which is used to describe the methanol plant in the optimization model. The investment cost for building the plant is obtained using a bottom-up approach, summing the cost of the main plant components.

An optimization model is developed, whereby the problem is identified as a Facility Location Problem, which is solved using a mixed integer linear programming (MILP) optimization model. The model solution provides the optimal location and the size of the methanol plants that minimize the total cost of the production system. The total cost comprises of the feedstock cost, the transport cost of biomass, the capital cost for building the production sites, the operation and maintenance (O&M) cost of the plant and the cost for transporting the bio-methanol to the ports. A detailed explanation concerning the methods used to determine the different cost components is given in chapter 5.

The following outputs are provided for each proposed scenario:

- optimal location of methanol production sites;

- size of the large-scale methanol synthesis plants, chosen among four different options: 100, 200, 300 or 400 MW1;
- amount of bio-methanol produced to meet the specified demand;
- final production cost of bio-methanol;
- an estimation of the GHG emissions reduction potential from replacing maritime fuels currently used in the Baltic area with bio-methanol.

The final objective of the optimization model is to minimize the aforementioned total cost of bio-methanol production for the 20 years simulation. Lastly, the Levelized Cost of Energy (LCOE) of bio-methanol is calculated for each scenario for comparison with the European market price of the main fuels used for maritime transport in Sweden. The LCOE accounts for all the production costs and considers the total amount of generated bio-methanol over the entire assumed lifetime of the plant, providing a cost indicator useful for the comparison with other technologies of different nature.

1.2 Literature review and research gap

Most of the research concerning the analysis of biofuel supply chains concentrates on economic implications. The optimization of a biofuel production network consists of a trade-off between limiting the costs for transporting the involved materials and reducing the investment cost of the required facilities [20]. The problem solution includes locating the facilities, determining the direction of the feedstock flows and defining the distribution of the final product.

A MILP model is a commonly used tool for the optimization of a biomass supply chain. Akgul et al. [21] applied MILP models to optimize a bioethanol supply chain by minimizing the total daily cost related to the operation of the entire supply chain. In their work, the model is applied to a case study of corn-based bioethanol production in Northern Italy, optimizing the location and size of the biorefineries, the distribution of the produced biofuel to the demand centres and the allocation of biomass resources to the different refineries. Tursun et al. [22] presented a multiperiod transhipment and facility location model to analyse the corn-based bioethanol refinery industry in Illinois. Leduc et al. [23] analysed the potential of producing methanol from harvested wood in Austria, for the purpose of blending with gasoline fuel. The study uses a MILP model to find the optimal location of the methanol plants that minimize the cost of methanol, calculated by considering the contribution of the costs related to biomass harvesting and transport, methanol production and transport and distribution of the final product. The proposed analysis also considered the effects of possible competition with conventional fossil fuels. Gunnarsson et al. [24] formulated a MILP model to optimize a forest fuel supply chain by minimizing the total cost of production, which includes biomass transport, pre-processing, purchase and storage. The model was applied on a real industrial case, considering one of the largest Swedish companies that supplies power plants with forest fuel. The authors used a heuristic solution approach to reduce the computational time required for solving the large obtained model. Leduc et al. [25] considered a case study of the Northern Sweden county of Norrbotten, applying a MILP model for optimizing the production of lignocellulosic based methanol, which is assumed to replace a portion of the gasoline consumed in the county for automotive transport purposes. In their study, they obtained the methanol cost for three different production plant sizes, 100, 200 and 400 MW. Also,

1 based on LHV of dry biomass input

they assessed the variation of methanol production cost induced by the integration district heat production at the plant.

Considering that little work has been done on investigating the economic aspects regarding the application of biofuels in the marine transport sector, this study applies a MILP model to optimize the production of lignocellulosic methanol to use for marine transportation purposes. The model is applied to a case study of Sweden, considering the energy demand for international and domestic marine transport and the availability of sawmill's by-products, which are the proposed feedstock. The optimization model is developed for multiperiod simulation, to account for variation in the energy demand. The research aims to minimize the cost of the supply chain, consisting of feedstock purchase, biomass transportation, plant capital investment, plant operation and maintenance and methanol distribution.

1.3 Thesis structure

The first two sections of this report introduce the current regulation regarding pollutants emission from marine transport applications, including an historical summary of the past regulations. In this phase, the fuels for marine transport commercially available in the Baltic sea are presented and the implications of the emissions regulation on the different fuel typologies are discussed.

Then, section 3 provides an outlook of the current situation regarding the global methanol production and presents a detailed description of the technologies considered for the conversion of woodchips and sawdust into methanol. The selected production process comprises of indirect biomass gasification, syngas cleaning and upgrade and low-pressure methanol synthesis. Following, the report revises the existing technologies that are considered mature for operating with methanol as fuel.

The subsequent chapter presents the Aspen Plus model built to simulate the bio-methanol plant. Indirect gasification, syngas cleaning and upgrade and methanol synthesis are described separately by listing the blocks involved in the modelling. Each section the relevant data and assumptions used for the simulation. The results obtained from the simulation are processed to retrieve the plant biomass-to-methanol conversion efficiency and the appliance's electricity consumption, which are relevant parameter needed for the optimization model.

The report continuous with the description of the optimization model that is implemented for the determination of the system configuration that minimize the total production cost of bio-methanol, described in section 5. This section presents the methods, data and assumptions used for describing the biomass supply chain, for estimating the capital and O&M costs of the plant and for determining the end-user's methanol demand. A summary of the modelling assumptions is presented in section 5.5. Subsequently, section 6 describes the method for determining the potential reduction of GHG emissions that can result from replacing fossil-based marine fuels with bio-methanol.

Before presenting the results obtained from the simulations, the considered scenarios are introduced in section 7, along with an explanation of the performed sensitivity analysis.

2 Emission standards regulation for marine transport and marine fuels

In addition to CO_2 emission limitations described in section 1, the maritime transport sector must comply with other emission standards concerning the generation of pollutants derived by the operation of internal combustion engines (ICEs). Emission standards for marine transport were first introduced by the International Maritime Organization (IMO) in 1978 with the "International Convention on the Prevention of Pollution from Ships", also known as MARPOL 73/78. The content of the Convention was amended by the "*1997 Protocol*", which in the Annex VI defined NOx and SOx emission standards for exhaust gases from ships known as Tier I [26]. After becoming effective in 2005, Annex VI was revised in 2008 introducing stricter emission limits (Tier II and III) [27]. The 2008 amendment was signed by 53 countries, counting roughly for 81.88% of the gross tonnage of the world's merchant fleet [28]. Table 2-1 summarizes the NOx emission standards introduced by the IMO during the past years. The limitations apply to any reciprocating ICE with rated capacity greater than 130 kW which is installed on a ship [26],[27]. The maximum allowed NOx level depends on the engine speed and the ship's construction year.

Table 2-1 *MARPOL Annex VI NOx emission limits [27]*

Emission Standard	**Construction Year**	**NO_x [g/kWh]**		
		n[1] < 130	130 ≤ n < 2 000	n ≥ 2 000
Tier I	2000	17.0	$45 \times n^{-0.2}$	9.8
Tier II	2011	14.4	$44 \times n^{-0.23}$	7.7
Tier III	2016	3.4	$9 \times n^{-0.2}$	1.96

With the 2008 amendments, fuel quality requirements regarding the sulphur content of the fuel oil were introduced to limit SOx emissions [27]. Currently, the maximum allowed sulphur content is 3.50% in weight which will be reduced to 0.50% starting from January 2020 [27]. Limitations are stricter for ships navigating through designated sea areas, referred as Emission Control Areas (ECAs). In such case, the maximum allowed sulphur content in the fuel is reduced to 0.10% in weight [27]. The Baltic sea area is included in the list of ECAs, making Sweden directly interested in developing low sulphur alternative fuels for marine transport.

Despite the international legislation effort aiming to reduce the environmental impact of shipping applications, the global marine transport sector is still highly dependent on fossil-based fuels. At present, the conventional marine fuels are petroleum derived products, which are commonly classified in two categories, residual fuels and distillates. The formers consist of products remaining after the petroleum refining process. These fuels are normally referred as FO and are classified according to kinematic viscosity. Intermediate fuel oils (IFOs) are the most common residual marine fuels used in the Baltic area, especially IFO380 and IFO180, where numbers indicate the fuel kinematic viscosity measured in centistokes. Distillates fuels are normally referred as marine gasoil (MGO), which represent any diesel fuel used for marine applications. Generally, marine diesel oil (MDO), fuels obtained by mixing MGO and FO, are also considered as distillate marine fuels.

[1] engine speed in rounds-per-minute (rpm)

Normally, IFO present a sulphur content below 3.5% and greater than 1%, considerably beyond the maximum allowed quantity imposed within ECAs. This allows the operation with such fuels in ECAs only if the propeller is retrofitted with an exhaust gas cleaning system able to reduce the emissions of SOx below the maximum allowed quantity. In alternative, ultra-low sulphur fuel oil (ULSFO) can be obtained from conventional FO after a desulphurization process, which reduces the sulphur content in the fuel below 0.1%.

The necessity of low sulphur fuels contributes to deviate the attention of the marine transport industry away from the conventional petroleum-based fuel, in advantage of cleaner alternatives. Fuels produced from natural gas, such as liquified natural gas (LNG) and methanol, are gradually increasing in popularity within the marine transport sector. Both LNG and methanol have the potential to reduce emissions of sulphur compounds over 90% and can decrease NOx emissions by 80% compared to petroleum-based fuels [29].

3 Biomass to methanol fuel conversion

This section initially presents a review of the global methanol demand and production, followed by a review of the methanol production process that was chosen for this study. Then, the chapter includes a collection of literature information regarding the properties of methanol as fuel and the advantages that bio-methanol introduces in terms of the reduction of pollutants in the exhaust gases

3.1 Methanol production

Methanol is a very important raw material for the chemical industry since it can be converted into a large variety of end-products. Figure 3-1 reports information regarding the different possible methanol end-uses and the partition of global methanol demand. The global methanol consumption amounted to 78 million tons in 2016, of which more than half was consumed in China (Figure 3-1), where from 2004 different local blending standards were introduced to define the methanol concentration in the methanol-gasoline blend [30].

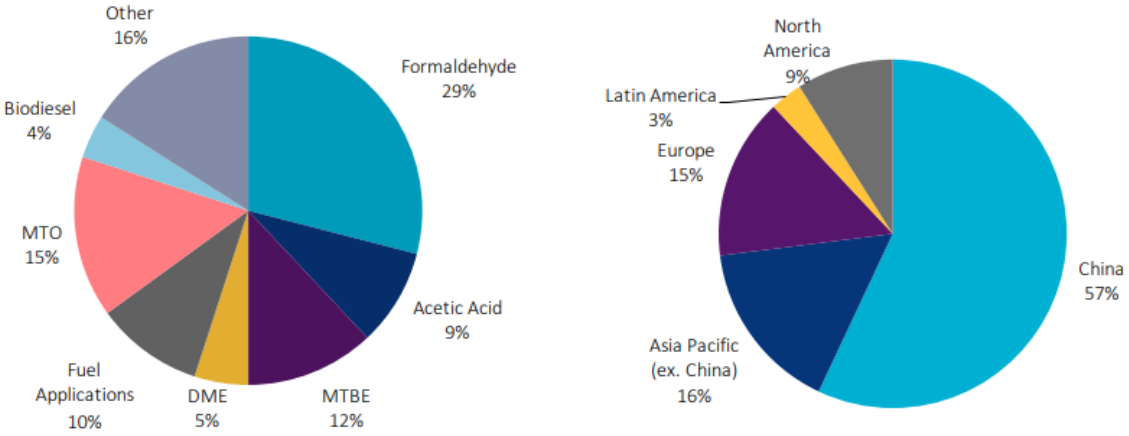

Figure 3-1 *Global methanol demand in 2015 by end-use (left) and by region (right) [30]*

Large shares of the global methanol consumption are related to the fuel market: 12% of the methanol consumption in 2016 was destined to the production of methyl tertiary-butyl ether (MTBE), which is used as a gasoline additive to increase the fuel octane number. Methanol is also involved in the biodiesel production process, which demanded 4% of the total methanol consumed during 2016. Furthermore, 5% of the methanol was converted to dimethyl ether (DME) and 10% was directly used as fuel for different applications.

At present, methanol is mainly synthetized from natural gas through a catalytic industrial process [31]. Natural gas represents the easiest raw material for the synthesis process and accounts for 90% of the global feedstock materials [32]. The use of natural gas in the recent years has been supported by the increased exploitation of unconventional gas resources, like shale gas, which heavily contributed to decrease the market price of natural gas. The methanol distillation process requires the natural gas to be converted into syngas, usually done through a steam reforming step [32].

Despite the popularity of natural gas as feedstock for methanol production, this alcohol can also be obtained by processing biomass following different conversion methods. If solid wood residues are considered as raw material, the conversion into a gaseous product through gasification would allow the use of the same methanol synthesis reactors involved in the

conventional process. Gasification is a proven and well-known technology that is commercially used worldwide [33], making it an option worth to consider for producing methanol from solid wood residues.

A few projects involving the production of bio-methanol from syngas obtained after gasification of woody biomass have been started in Sweden during the past years. In 2010, a pilot plant for production of bio-DME and bio-methanol was built in Piteå (Sweden). The demonstration plant, owned by the Swedish biofuel company Chemrec AB, has a production capacity of 1300 tons per year and uses black liquor from Domsjö Fabriker's pulp mill as feedstock [34]. Two more Swedish companies announced project aimed to the construction of a bio-methanol production plant. The forest-owner association Södra announced in 2017 the intention of building a plant to produce 5000 tons of bio-methanol per year, situated at its pulp mill in Mönsterås and predicted to start operation in 2019 [35]. VärmlandsMetanol AB is currently engaged in a project for building a bio-methanol synthesis plant using solid wood as feedstock [36]. The plant will be built in Hagfors (Sweden) and will have a production capacity of 315 tons of methanol per day [37].

3.1.1 Methanol from woody biomass

To be converted into methanol, solid biomass must first be reduced into gaseous form through a gasification process. Given its high content of water, solid wood must be dried to reduce the moisture content to approximately 15% before entering the gasifier reactor. The obtained syngas, a mixture of carbon monoxide (CO), carbon dioxide (CO_2), hydrogen (H_2), water (H_2O) and methane (CH_4), must be treated to obtain a final chemical composition suitable for the methanol synthesis process. The characteristics and requirements of the different processes involved in a wood-to-methanol plant are described in the following sections.

Gasification

Gasification is a thermochemical conversion process which allows to transform a solid (or liquid) fuel into a gas (or vapor) phase and a solid phase. The purpose of gasification is to obtain a final gaseous product, called syngas, with a higher heating value than the feeding fuel and a greater hydrogen to carbon ratio [38]. The generated syngas can then be used for energy production purposes or for production of chemicals and transport fuels. The remaining solid phase is referred as char and represents the unconverted carbon and the inert material that were originally contained in the feedstock material.

The process consists in the partial oxidation of the carbon contained in the starting fuel, through the reaction with a gasifying agent which can be either air, oxygen, hydrogen, steam or carbon dioxide. The selection of the gasification medium strongly affects the final chemical composition of the syngas, making it an important design parameter that must be chosen accordingly to the end-use decided for the syngas. As shown in Figure 3-2, using steam as gasification agent leads to an increase of the hydrogen content in the product gas and so to a greater hydrogen-to-carbon ratio. On the other hand, gasification with pure oxygen will increase the presence of CO and CO_2 in the syngas. However, if too much oxygen is provided to the reactor, gasification turns into a combustion process and the obtained gas phase won't contain any remaining heating value. Generally, gasification with oxygen generates a syngas with higher heating content compared to the steam gasification process [38].

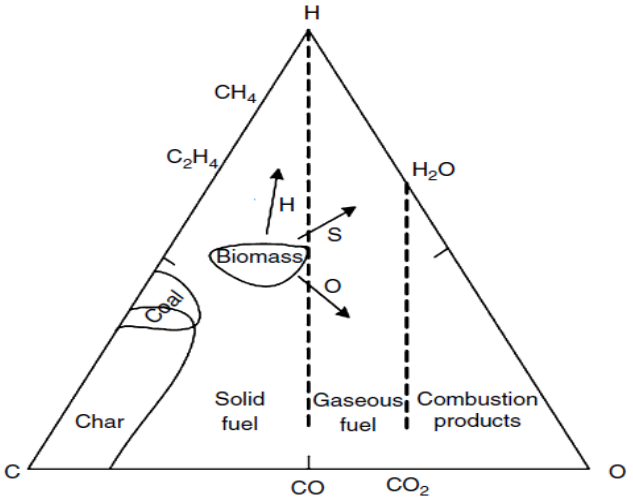

Figure 3-2 *C-H-O ternary diagram[1] of gasification process with steam (S), hydrogen (H) and oxygen (O) [38]*

Gasification develops following four main steps:

- oxidation
- drying
- pyrolysis
- reduction

The oxidation step provides the heat needed for the endothermic phases of the gasification process and to maintain the temperature in the reactor at the required level. The necessary thermal energy is produced by three exothermic combustion reactions:

$$C + O_2 \rightarrow CO_2 \ (\Delta H = -394 \text{ kJ/mol}) \quad (3.1)$$

$$C + \frac{1}{2}O_2 \rightarrow CO \ (\Delta H = -111 \text{ kJ/mol}) \quad (3.2)$$

$$H_2 + \frac{1}{2}O_2 \rightarrow H_2O \ (\Delta H = -242 \text{ kJ/mol}) \quad (3.3)$$

The oxidation reactions develop in shortage of oxygen to avoid the complete combustion of the fuel. The produced gas is a mixture of CO_2, CO, H_2O and nitrogen (only if air is used as gasification agent).

During the drying phase the moisture contained in the future is evaporated. The thermal energy required by the process depends on the moisture content of the feeding fuel, which should be contained between 10 and 20% through a pre-drying process in order to limit the amount of energy needed by the gasification drying step [38]. An elevated moisture content in the feed fuel will lead to a gas product of reduced heating value.

1 tool for representing biomass conversion processes. It indicates the concentration of the three represented elements (carbon, oxygen and hydrogen) in the considered product. The corners are the pure elements (100% concentration), while a point within the triangle represent a ternary mixture of the three substances.

Pyrolysis is a thermochemical decomposition process that involves the breakdown of the heavy hydrocarbon molecules of the biomass into lighter molecules. The dried fuel is decomposed into solid, liquid and gaseous fractions though a series of endothermic reactions that can be summarized with the overall reaction (3.4).

$$dry\ biomass \rightarrow H_2 + CO + CO_2 + H_2O_{(g)} + light\ hydrocarbons^1 + \\ + tar_{(l)} + char_{(s)}\ [39] \quad (3.4)$$

The chain of reactions develops at temperatures ranging between 250 °C and 700 °C, without involving any major chemical interaction with the gasification agent [38]. The composition of the pyrolysis product is variable and depends on the configuration of the gasifier reactor [39]. Generally, 70-90% in weight of the fed material is converted into gaseous mixture of CO_2, CO, H_2 and light hydrocarbons (e.g. CH_4) [39].

The reduction step involves the products formed through the pyrolysis and drying phases. The remaining char and the generated gas mixture react to form the final syngas according to the following reactions:

$C + CO_2 \rightarrow 2CO$ (Boudouard reaction, ΔH = 172 kJ/mol) (3.5)

$C + H_2O \rightarrow CO + H_2$ (water-gas reforming, ΔH =131 kJ/mol) (3.6)

$CO + H_2O \rightarrow CO_2 + H_2$ (water-gas shift reaction, ΔH = -41 kJ/mol) (3.7)

$C + 2H_2 \rightarrow CH_4$ (methanation reaction, ΔH = -75 kJ/mol) (3.8)

Despite reaction (3.7) and (3.8) are exothermic, the overall process is endothermic and so it demands part of the thermal energy released by the oxidation reactions (3.1), (3.2) and (3.3). According to Le Chatelier's principle, the endothermic reactions (3.5) and (3.6) are favoured by an increase of the reduction temperature, while reactions (3.7) and (3.8) increases the yield of products at lower temperatures. Hence, the final composition of the syngas is strongly dependant on the temperature of the reduction step.

Other than affecting the equilibrium of the reactions involved in the reduction step, the operating temperature has an impact on the whole gasification process. At higher temperatures, the char conversion is improved due to an increase of the char oxidation. As consequence, solid residues are reduced but so it's the final heating value of the produced syngas. Increasing the reduction temperature also allows to reduce the formation of tar but enhance the risk of ash sintering in the process. The described effects are summarized in Figure 3-3. As result, different configurations of the gasification reactor were developed for operation at different temperature levels, in order to obtained the desired combination of syngas composition and amount of residues. The most diffused configurations for a biomass gasification reactor are: entrained flow reactor, fixed bed, fluidized bed, rotary kiln reactor and plasma reactor [39]. For the processes that have been implemented at full scale, the typical gasification temperature ranges between 800 °C and 1100 °C [39].

[1] CH_4, C_2 and C_3

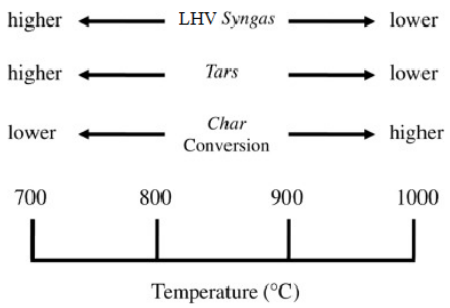

Figure 3-3 *Effect of the gasification temperature on the obtained products [39]*

The gasification reactors that have been primarily investigated for production of bio-syngas are the pressurized direct oxygen fired gasifier and the atmospheric indirect steam-blown gasifier, which are schematically represented in Figure 3-4 [40]. The model developed by Heyne et al. [40] based on the exergy efficiency of the process, showed that pressurized direct gasification guarantees slightly higher efficiencies than indirect gasification [40]. However, direct gasification leads to larger amount of CO_2 in the product gas, which represent a disadvantage for synthesis processes that requires CO_2 separation [40]. In this case, there aren't significant differences in performances between the two configurations [40]. Indirect gasification allows better carbon conversion, which makes it a preferable technology when methanol production is the final purpose of the process [40].

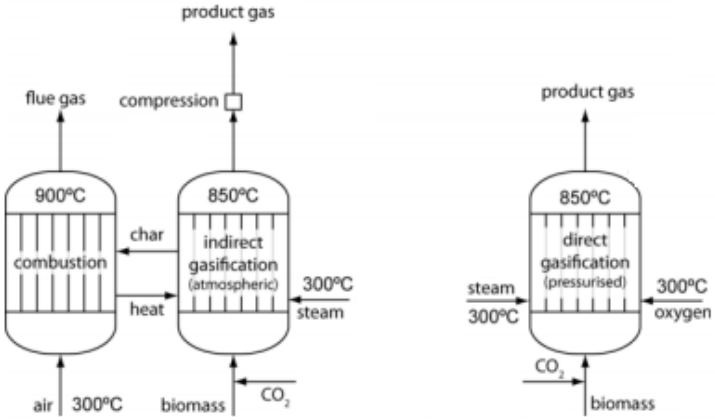

Figure 3-4 *Atmospheric steam-blown indirect gasifier (left) and pressurized direct oxygen fired gasifier (right) (modified from [40])*

Syngas cleaning and upgrading

The syngas produced by the gasification process contains contaminants that must be removed to avoid complications with the downstream methanol synthesis equipment. There are hazardous contaminants that directly come with the feedstock material (e.g. ash, nitrogen, sulphur compounds) and others that are results of the gasification process and of incomplete gasification (e.g. tar, char). Table 3-1 reports the typical contaminants limits for the methanol synthesis process.

Table 3-1 *Syngas contaminants requirements for methanol synthesis [41]*

Particulate[1]	Tars	Sulphur	Nitrogen
< 0.02 mg/m3	< 0.1 mg/m3	< 1 mg/m3	< 0.1 mg/m^3

[1] includes soot, dust, char and ash

One way to reduce the presence of contaminants in the syngas is to apply techniques aiming to reduce their formation inside the gasification reactor. These approaches are referred as primary methods, while the technologies that allow the clean-up of the syngas outside the gasifier are indicated as secondary methods. Depending on the temperature of the cleaning process, the secondary methods can be classified into hot or cold clean-up processes. The formers are generally identified as technologies operating at temperatures ranging between 400 °C and 1300 °C [41], making them attractive because they allow to avoid the cooling and reheating of the syngas.

The size and composition of the particulate matter leaving the gasifier depends on the feedstock material and on the gasification process itself. The particles can be as little as 1 μm or exceed 100 μm [41]. The particulate mainly includes the inorganic fraction of the biomass and solid carbon remained after the gasification [41]. Different technologies are available for particulate removal, the most diffused are cyclones, barrier filters, electrostatic precipitators and wet scrubbers. Given the size of the particles involved and considering the required separation efficiency, barrier filters are a suitable option for the considered application. The technology allows the collection of particulate matter of 0.5 to 100 μm in size at removal efficiencies higher than 90% [42]. The solid particles are separated from the gas by forcing its passage through a porous material. Depending on the selected filter material, barrier filters can be applied at temperatures ranging from 150 °C to 750 °C [42].

Tar identifies all the organic contaminants with a molecular weight greater than benzene [43]. As mentioned in section *Gasification*0, the formation of tar depends on the chosen gasifier configuration and on the gasification temperature. Among all the gasifiers, downdraft gasifiers allow the lowest tar concentration in the syngas (less than 1% in weight) while updraft gasification reactors can lead to a tar content as high as 20% in weight [39]. The tar content in the syngas can be reduced through physical or chemical methods. Since tar condenses at rather low temperatures (250 to 300 °C [39]), it is possible to physically separate the tar particles from the syngas once the syngas temperature is reduced. The physical separation can be done either in wet or dry conditions, with the former being a mature technology and guaranteeing better removal efficiencies [44]. The advantage brought by dry methods is the possibility to remove tars with the same equipment used for particles removal [44]. Chemical methods involve the cracking of tar particles by using a catalyst (catalytic cracking) or at high temperatures (thermal cracking). Catalytic cracking can be pursued either downstream or inside the gasifier. The possibility to reduce tar formation directly inside the gasifier results very attractive since it eliminates the necessity of downstream cleaning equipment, therefore several studies have been conducted with the purpose to analyse the effect of different catalyst on tar formation and on the composition and heating value of the final product [43]. Dolomite has been widely investigated as catalyst for tar cracking in fluidized bed gasifiers, showing positive results in terms of tar reduction without affecting the heating value of the product gas [43].

Sulphur contaminants are mainly present in form of hydrogen sulphide (H_2S) with lower concentrations of carbonyl sulphide (COS) [41], both originating from the sulphur contained in the fed fuel. Even though woody biomass might contain little amounts of sulphur, a removal step might be needed to ensure the respect of the maximum concentration level for methanol synthesis. The presence of acid compounds represents a risk in terms of catalyst poisoning for the methanol synthesis [32]. Nowadays, absorption processes based on sulphur removal with liquid agents are the best fit for large-scale industrial applications [32]. The

Rectisol™ process, using methanol as solvent, is the preferred technology for sulphur removal from syngas destined to methanol production in large-scale plants [32]. The process allows the highest sulphur removal efficiency among all the other available technologies, reducing the concentrations of H_2S and COS to as low as 0.1 ppmv[1] each [32].

After removing the impurities, the chemical composition of the syngas must be adjusted to what required by the methanol synthesis process (see section *Methanol synthesis*). The hydrocarbons in the syngas must be converted to H_2 and CO, which can be done either through steam reforming or auto thermal reforming. The process is represented by the endothermic chemical reaction (3.9).

$$CH_4 + H_2O_{(g)} \rightarrow 3H_2 + CO \text{ (steam-methane reforming reaction, } \Delta H = 206 \text{ kJ/kmol)} \quad (3.9)$$

Then, the hydrogen to carbon monoxide ratio (H_2/CO) is brought to the desired level by converting CO to H_2 and CO_2 through a high-temperature water-gas shift (WGS) process (equation 3.7). The syngas stream is usually split before the WGS reactor, only part of the syngas is processed in order to obtain the H_2/CO required for methanol synthesis (see section *Methanol synthesis*) [32].

Lastly, the syngas undergoes another upgrading step to partially remove CO_2 before being sent to the methanol synthesis unit. CO_2 is removed with the other acid compounds (H_2S and COS) with the Rectisol™ process. Methanol absorption properties are function of the absorption temperature, which can be adjusted to favour the removal of sulphur compounds rather than CO_2.

Methanol synthesis

Reactions (3.10) and (3.11) summarize the methanol synthesis process, where CO_2 and CO react with H_2 producing methanol and water as by-product. The WGS reaction (3.7) binds the two methanol synthesis reactions. The indicated enthalpies of reaction refer to the standard state temperature condition (298 K) and to a pressure of 50 bar. Since both reactions are exothermic and lead to a reduction of number molecules, the equilibrium can be moved towards the product by reducing the temperature and increasing the pressure as indicated by Le Chatelier's principle.

$$CO + 2H_2 \rightarrow CH_3OH \text{ (hydrogenation of CO, } \Delta H = -90.7 \text{ kJ/mol)} \quad (3.10)$$

$$CO_2 + 3H_2 \rightarrow CH_3OH + H_2O \text{ (hydrogenation of } CO_2\text{, } \Delta H = -40.9 \text{ kJ/kmol)} \quad (3.11)$$

According to reactions (3.10) and (3.11), the stoichiometric number (SN) of the fed syngas, defined in equation (3.12), should be equal to two. However, it has been reported that a slightly higher SN (from 2.05 to 2.08) benefits the efficiency of the methanol production process due to an increase of the catalyst performance [32]. Therefore, the upgrading of syngas should lead to a final H_2/CO around two.

$$SN = \frac{[H_2] - [CO_2]}{[CO] - [CO_2]} \quad (3.12)$$

[1] parts per million by volume

Despite the chemistry of the involved reactions suggests a synthesis process at high pressures, the development of the syngas cleaning technologies allowed the application of more active catalysts which lead to a reduction of pressure compared to the first designed methanol synthesis processes. The operating pressure has been reduced from the initial level of 250-300 bar to 50-100 bar [45]. The possibility of operating at low pressure and low temperature (220-275 °C) allowed a great reduction of the material cost of the reactor [45]. The most common catalyst used in commercial applications is the Copper-Zinc Oxide-Aluminium Oxide ($Cu\text{-}ZnO\text{-}Al_2O_3$) catalyst, which can guarantee up to 5 years of lifetime under normal operating conditions [45]. Other than controlling the concentration of contaminants in the syngas (as reported in section *Syngas cleaning and upgrading*), it is important to maintain the temperature in the synthesis reactor below 300 °C to avoid the deactivation of the catalyst by sintering [45].

Reactors for methanol synthesis can be either adiabatic or isothermal. The former design doesn't imply the presence of an external cooling system, therefore the reaction temperature is controlled either by feeding cold syngas at different stages inside the reactor (quench reactor) or by indirect intercooling with water as cooling medium. Temperature control inside adiabatic reactors results challenging and catalyst sintering might occur [45]. On the other hand, isothermal reactors allow a stable temperature control through the indirect cooling of the reactor shell. The isothermal design introduces many advantages over the adiabatic design thanks to the better temperature control, including longer catalyst lifetime, higher methanol yield and the possibility to recover the energy absorbed by the coolant for power generation purposes [45]. Due to their simpler design, adiabatic reactors are preferred over isothermal reactors for small scale applications [45]. Figure 3-5 gives a schematic representation of the different methanol reactors currently available.

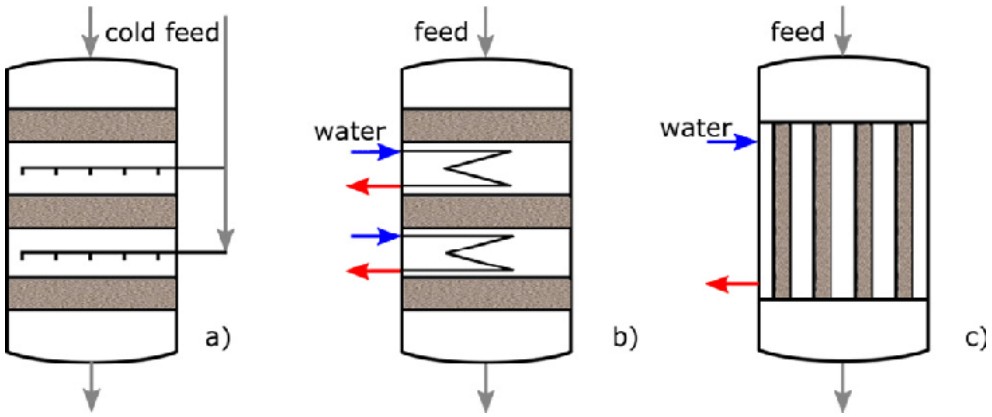

Figure 3-5 *Quench (a), adiabatic with indirect cooling (b) and isothermal (c) reactors for methanol synthesis [45]*

The product obtained from the synthesis reactor must be sent to a distillation plant to separate the methanol from the other species (water vapour, ethanol, higher alcohols, ketones and ethers) [45]. In order to increase the conversion efficiency of the process, the unreacted syngas is recirculated in the synthesis reactor.

3.2 Methanol use as fuel

Despite being able to guarantee the highest thermal efficiency among any practical ICE [46], conventional FO operation in CI engines introduce disadvantages in terms of pollutant emissions. NOx and PM emissions are high and the simultaneous reduction of the two requires

the use of complicated technologies, such as a post-combustion selective catalytic reduction treatment [47]. While emission standards introduce tightening emission limits (please refer to section 2), the interest on alternative fuels able to lower CO_2 and pollutants emissions is increasing. Methanol has the potential to lower tailpipe emissions of NOx and PM due to high oxygen and low sulphur concentrations, which induce cleaner burning characteristics [47].

Ships are normally propelled by CI engines, making the application with methanol challenging due to the low cetane number compared to conventional FO, as reported in Table 3-2. Due to its scarce auto-ignitibility, methanol must be blended with a fuel with better auto-ignitibility properties or with an ignition improver to make possible the operation in a CI engine. There are two main approaches for the solution of this problem:

- mix the methanol with conventional fuel oil, followed by direct injection of the blend in the engine cylinders;
- use a separate injection dual fuel (DF) approach.

If the first approach is chosen, emulsifier agents or co-solvents must be added to the blend to overcome the miscibility problems between oil derived fuels and methanol [48]. However, the maximum possible methanol concentration in the blend remains low [48]. For operation with a methanol-diesel blend containing 20% in weight of methanol, NOx formation isn't reduced compared to the operation with the conventional fossil fuel [49].

Table 3-2 *Comparison of methanol and HFO fuel properties [50],[51]*

Property	**Methanol**	**FO**
Cetane number	3	35
Density at 25°C [kg/m^3]	792	900 - 1010
Kinematic Viscosity [mm^2/s]	0.75 (at 20°C)	66.6 (at 80°C)
LHV [MJ/kg]	19.7	41.1
H/C [mol/mol]	3.97	2.06
Oxygen content [%wt]	50	0
Sulphur content [ppm wt]	0	8300
Stoichiometric air/fuel ratio	6.45	13.8

A DF engine configuration allows to increase the utilization ratio of methanol and simultaneously reduce NOx and PM formation without incurring in any mixability problems, since methanol and FO are separately introduced in the cylinder [48]. Methanol can be directly introduced in the combustion chamber or through a carburettor, following the fumigation approach [50]. In the first case, the methanol is ignited by a pilot flame which is developed by the combustion of the secondary fuel injection. This approach requires strong modifications to the engine injection system [48], therefore it is an alternative solution to the conventional CI engine rather than an option for retrofitting existing propellers. On the other hand, the fumigation approach can be followed when considering the retrofitting option, which is of peculiar interest for those applications that generally require a long lifetime, like marine engines [48]. Several studies have been conducted about the effect of methanol fumigation on the engine operation, reporting the relevancy of the methanol utilization ratio. The reduction of NOx in DF operation was demonstrated to improve when the methanol ratio is increased [48].

The DF engine designed for methanol operation is a commercially available solution which has already been involved in few demonstration projects related to the shipping industry. The 1500 passengers ferry Stena Germanica has been converted to methanol operation and is currently operating, powered with four 6 MW DF engines provided by Wärstilä [52], [53]. Stena Line announced its commitment to support the production and the use of bio-methanol in the marine industry [53]. The company reported that the conversion of Stena Germanica costed approximately 450 k€/MW [53]. The Canadian company Waterfront Shipping Company Ltd announced in 2013 a partnership with three other fellow shipping companies (Marinvest, MOL and WL) to introduced new methanol vessels powered by MAN's DF engines [54]. The company currently counts seven methanol vessels in its fleet, with the first introduced in April 2016 already recording more than 3000 hours running on clean methanol [54]. However, methanol market price is still twice as high as conventional FO [55], challenging the large penetration of the fuel in the shipping industry.

4 Data and methods for modelling the methanol synthesis plant

Wood chips and sawdust are modelled in Aspen Plus as a non-conventional solid material by defining the ultimate and proximate analysis indicated in Table 4-1. It is assumed that the feedstock is received wet, having a moisture content of 50%$_{wt}$ and lower heating value (LHV) of 19 MJ/kg [56].

Table 4-1 *Ultimate and proximate analysis of biomass feedstock [56]*

Moisture	50%
Ultimate analysis [%$_{wt}$, dry]	
C	51.19
Cl_2	0.05
H_2	6.08
N_2	0.20
S	0.02
O_2	41.30
Ash	1.16
Proximate analysis [%$_{wt}$, dry-ash free]	
Volatile matter	80.94
Fixed carbon	19.06

Following is a list of the general assumptions used in the model:

- The process is steady state.
- All gases are ideal.
- Air is modelled as 79%$_{mol}$ N_2 and 21%$_{mol}$ O_2.
- Pressure loss in heat exchanger is 2% unless differently specified.
- 80% isentropic efficiency of compressors.
- 98% mechanical and electrical driver efficiency.
- 85% isentropic efficiency of pumps.
- Heat and pressure losses in the reactors are neglected unless differently specified.
- The selected fluid-dynamic property model is Peng-Robinson.
- Electricity cost

The assumed cost of electricity is referenced to electricity price registered in Sweden for industrial consumers of standard consumption band IF[1] during the second semester of year 2016 [57]. The previously reported cost is increased by 20% to account for VAT.

4.1 Gasification unit

Before being introduced in the gasifier, the feedstock is dried for reducing the moisture content to 15%$_{wt}$. The drying process is modelled using a reactor block, a separator and two heat exchangers. The reactor DRYER, using a calculator block, reduces to 15% the moisture content of the received non-conventional wood stream. Then, the water is separated from the remaining feedstock in the separator block SEP and sent to heat exchanger HX-D1. All the

[1] annual electricity consumption between 70000 and 150000 MWh

water received by HX-D1 is evaporated, leaving the heat exchanger as saturated vapour at atmospheric pressure. The energy needed for the evaporation process is provided by HX-D2, which cools a stream of pre-heated air from 70 °C to 20 °C. Design specification AIR-DRY (Table A-1) is defined to calculate the mass flow of air that guarantees the final conditions imposed for the streams of evaporating water and cooling air. Moreover, blocks DRYER and HX-D1 are energy integrated by the energy stream Q-DRYER. The drying air stream is subjected to a 5% pressure loss during the process. The compressor C-DRY produces the work necessary to overcome this loss. The electrical power consumed by C-DRY is accounted as operation cost of the plant. The dried biomass is fed to the block PYROL to simulate the instant drying and pyrolysis of the fuel. In this process, the biomass is separated into its constituent components, according to the ultimate analysis specified in Table 4-1. The outlet stream is divided into three material streams by the separator column SEP-1. The mass flow rate of each stream is defined through a calculator block, allowing the separation of ashes and char from the volatile matter. It is assumed that all the fixed carbon contained in the biomass converts into char, which is directed to block COMB to model the char combustion process. The air flow entering the reactor is calculated using design specification AIR-COMB (Table A-2) and considering an air excess of 20% compared to stoichiometric conditions. The energy stream Q-COMB models the energy transferred from the char combustion chamber to the gasification reactor. Furthermore, the char combustion temperature is determined with a design specification T-COMB (Table A-3) to achieve a gasification temperature of 850 °C. The volatiles enter the stoichiometric reactor R-1. In this block, S, N and Cl react with H_2 to form H_2S, NH_3 and HCl respectively. Subsequently, these obtained products are separated from C, O_2, H_2 and H_2O, which are fed in reactor block GASIFIER. This reactor operates at atmospheric pressure and 850 °C, and has a defined yields distribution, determining the molar fraction of each component obtained after the block. The yield is fixed to obtain the gas composition defined in Table 4-2.

Table 4-2 *Composition of product gas obtained after gasification [58]*

Product	**[$\%_{mol}$, wet]**
H_2O	0.199
H_2	0.167
CO	0.371
CO_2	0.089
CH_4	0.126
C_2H_4	0.042
C_2H_6	0.006

The gasifying steam is added to GASIFIER at 1 bar and 300 °C. A calculator block imposes that 0.019 kg of steam are fed for each kilogram of dry biomass [58]. Blocks PYROL and R-1 are energy integrated with the gasification reactor by the energy streams Q-PYROL and Q-R1 respectively. Lastly, the main gas stream GAS-PROD is mixed with stream R1-SYN, which was previously separated from the main gas flow by SEP-2.

The Aspen Plus simulation flowsheet of the gasification process is displayed in Figure B-1, while Table 4-3 reports a short description of the included blocks.

Table 4-3 *Description of blocks used for modelling biomass gasification*

Name	Block	Description
DRYER	RStoic	Reduces moisture content in the biomass to 15%
SEP	Sep	Separate the dried biomass from the dried water
HX-D1	Heater	Evaporates the water separated from the biomass
HX-D2	Heater	Cools the air used for drying the biomass from 70 to 20 °C
C-DRY	Compr	Blower fan for circulating the air necessary to dry the biomass
PYROL	RYield	Simulates instant drying and pyrolysis of biomass
SEP-1	Sep	Divides ash, char and volatiles
R-1	RStoic	Converts S, N and Cl to H_2S, NH_3 and HCl respectively
SEP-2	Sep	Separates H_2S, NH_3 and HCl from the other gas components
COMB	RStoich	Models char combustion
HX-AIRPH	Heater	Preheats the air before injection in the char combustor
C-COMB	Compr	Provides to the air stream the necessary energy to overcome pressure losses in the air preheater
GASIFIER	RYield	Models the gasification process
HX-STEAG	Heater	Produces steam at 300 °C required for the gasification process
MIX-G1	Mixer	Mixes gas products obtained from gasification with products from R-1

4.2 Syngas upgrade

This part aims to model the processes required to upgrade the gas obtained from gasification to a high-quality syngas that can be used for methanol synthesis. The gas requirements for the methanol synthesis process are described in sections *Syngas cleaning and upgrading* and *Methanol synthesis*.

The gas is cooled to 250 °C before the particulate removal phase, which is modelled as a 2% pressure drop. Then, the temperature of the gas stream is further reduced to 70 °C, to allow the cleaning from impurities such as tars (C_2H_4 and C_2H_6), NH_3, HCl and H_2S. The elimination of these compounds is modelled with the separator column SEP-3, which also enforces a 5% pressure drop on the gas stream. A more detailed approach for modelling the different processes involved is possible, but not considered an objective of this study. Before the described gas cleaning phases, block C-S1 pressurizes the gas stream to ensure that the gas pressure never drops below the atmospheric level. Once the impurities are eliminated, the pressure and temperature of the gas are adjusted in blocks C-S2 and HX-S3 respectively, to reach the conditions for the steam reforming process. The gas stream, which contains CO_2, CO, CH_4, H_2 and H_2O enters the Gibbs free energy minimization reactor REFORMER at 30 bar and 850 °C. In this reactor, CO_2, CO, H_2 and H_2O are fixed as possible products. Therefore, all the CH_4 contained in the gas stream is reformed. The gas temperature remains unchanged after leaving the reactor, while pressure reduces by 5% compare to the entry level. Steam is added into REFORMER at 30 bar and 400 °C, and design specification WAT-REF
(

Table A-4) calculates the steam mass flow that ensures a molar ratio of 1.5 between injected steam and methane in the reactor. Subsequently, the stream is cooled to 350 °C by HX-S4 before being directed to the split block BYPASS, which directs a fraction of the incoming gas towards block WGS. This unit models the WGS process using an adiabatic Gibbs free energy minimization reactor, defining the restricted equilibrium for the water-gas shift reaction (2.7) and imposing a 100% conversion for the incoming CO. Steam at 400 °C is added to block WGS, and design specification WAT-WGS (Table A-5) calculates the mass of injected steam. Compressor C-S3 makes-up for the 5% pressure loss introduced by block WGS, bringing the pressure of stream SHIFT-P to the same level as stream SKIP-WGS before they are mixed in block MIX-S1. Then, the mixed stream is cooled to 30 °C and directed to the separator column RECTISOL, which simulates the effect of the Rectisol™ process by separating 99% of the CO_2 from the treated gas. As for the gas cleaning processes, the CO_2 stripping could be modelled in a more detailed way, which is not the scope of this study. Design specification BP-RATIO (

Table A-6) calculates the fraction of product gas that must by-pass the WGS reactor in order to obtain a SN of 1.80 after the CO_2 separation step. Lastly, the upgraded syngas is compressed by block C-M1 to the pressure level required for the methanol synthesis process.

Figure B-3 shows the Aspen Plus flowsheet for the simulation of the syngas upgrade process, and Table 4-4 lists the included blocks.

Table 4-4 *Description of blocks included in the syngas upgrade model*

Name	Block	Description
C-S1	Compr	Used to pressurize the product gas before the cleaning steps
HX-S1	Heater	Reduces the temperature of the product gas to 250 °C, before being sent to the particulate filter system
PART-FIL	Valve	Simulate particle separation as a 2% pressure loss
HX-S2	Heater	Cools the product gas to 70 °C, as required for the cleaning processes
SEP-3	Sep	Separates NH_3, HCl, H_2S, C_2H_4 and C_2H_6 from the product gas stream
C-S2	Compr	Compresses the syngas for the reforming process
HX-S3	Heater	Increases the gas temperature to 850 °C
REFORMER	RGibbs	Steam reforming reactor, operates at 850 °C and 30 bar
PUMP-R	Pump	Compresses water for the steam reforming process
HX-REF	Heater	Produces steam at 400 °C to use in the REFORMER reactor
HX-S4	Heater	Cools the reformed gas stream to 350 °C
BYPASS	FSplit	Directs part of the reformed gas to the WGS reactor
WGS	RGibbs	WGS reactor. It converts all the received CO to H_2
PUMP-WGS	Pump	Compresses the water to use in the WGS reactor
HX-WGS	Heater	Converts the incoming stream of pressurized water into steam at 400 °C to use in the WGS reactor
C-S3	Compr	Restores the pressure of the shifted gas stream to the same level as the reformed gas stream that by-passed the WGS reactor
MIX-S1	Mixer	Reconnects the streams that were previously separated by BYPASS
HX-S5	Heater	Cools the syngas to 30 °C before the Rectisol™ process
RECTISOL	Sep	Simulates the effect of a Rectisol™ unit by separating 99% of the CO_2 from the received syngas

4.3 Methanol synthesis

The isothermal methanol synthesis reactor is modelled with Gibbs free energy minimization block M-REACT, assuming a reaction temperature of 250 °C and 90 bar pressure inside the reactor. Also, the reactor introduces a pressure loss of 5 bar. Methanol, CO_2, CO, H_2 and H_2O are identified as possible product that can be obtained at the block outlet. Reactions (2.7), (2.10) and (2.11) are indicated to define the restricted equilibrium of the reactor block. Then, the product is cooled to 50 °C, and condensed methanol and water are separated from the remaining gaseous unreacted elements in the separator column SEP-M1. A portion of this unreacted gas is directly recirculated inside block M-REACT after the pressure level is

restored to the same pressure as stream MIXED by compressor C-M2. Design specification GAS-REC (Table A-7) calculates the split fraction of block SPLIT-1 that allows the maximum recirculation of unreacted gas without increasing the molar fraction of CO_2 over 3% for the stream fed in M-REACT. The remaining unreacted products are fed to separator column H2SEP, which models a hydrogen separation membrane. The recovered hydrogen is partially recirculated, compressed in block C-M3 and mixed with the stream of high pressure upgraded syngas. The mass flow of recirculated hydrogen is calculated with design specification H2-REC (Table A-8), which limits the recovery to the amount that produces a SN equal to 2.05 for stream MIX1. The crude methanol leaving SEP-1 is depressurized to atmospheric level by valve V-M1. Then, the crude methanol enters distillation column DIST, where pure methanol is recovered from the mixture.
Table 4-5 reports the list of blocks used for the simulation of methanol synthesis, while a full representation of the flowsheet is displayed in Figure B-2.

Table 4-5 *Description of blocks used for modelling the methanol synthesis process*

Name	Block	Description
C-M1	Compr	Compresses the upgraded syngas directed to the synthesis process
MIX-M1	Mixer	Mixes the upgraded syngas with the hydrogen recovered from the unreacted gas
C-M3	Compr	Increases the pressure of the recovered hydrogen stream to the same level as the pressurized upgraded syngas
H2SPLIT	FSplit	Recirculate a portion of the recovered hydrogen to obtain SN=2.05 in the stream MIX1
H2SEP	Sep	Separate the H_2 contained in the received stream
SPLIT-1	FSplit	Recirculates a portion of the unreacted gases, without increasing over 3% the molar concentration of CO_2 inside the treated gas
C-M2	Compr	Restore the pressure of the recirculating unreacted gas to the same pressure of stream MIX1
MIX-M2	Mixer	Mixes the recirculated unreacted gases with the fresh syngas
HX-M1	Heater	Heats up the incoming gas stream to 250 °C
M-REACT	RGibbs	Methanol synthesis reactor, operates at 250 °C and 90 bar. Introduces pressure loss of 5 bar.
HX-M2	Heater	Cools the gas stream to 50 °C to condense methanol and water
SEP-M1	Sep	Separate crude methanol from the unreacted gases
V-M1	Valve	Reduces the pressure of the gas stream to atmospheric level
DIST	DSTWU	Distillates pure methanol

5 Optimization model for defining methanol plant locations

Due to the low bulk and energy density of wood chips and sawdust, their transport results rather expensive since the transported capacity is not limited by the weight of the carried load but by its volume [59]. Thus, the final production cost of bio-methanol is strongly influenced by the location of the production plants. This chapter describes how the methanol

production chain has been modelled, data and assumptions used in the simulation and presents the mathematical equations that define the MILP optimization model, which aims to identify the optimal location of the bio-methanol plants that minimize the total cost of production. The production chain is divided as: biomass supply, methanol production plant and end-users demand.

5.1 Biomass supply

The feedstock material examined within this study includes wood chips and sawdust, considered as by-products of the sawmilling process. Thus, the geographical position and production capacity of sawmills in Sweden were collected so to identify the stakeholders within the biomass supply chain [60]. Only sawmills having an annual production capacity greater than 30000 m^3 are reviewed in this study. A list reporting the location and production capacity of the considered sawmills is provided in Appendix .

Of the 179 Swedish sawmills, 116 match the enforced production capacity requirement [60]. This limitation has been introduced to reduce the number of variables included in the MILP optimization model, assuming that small sawmills are less likely to have the investment capacity required for the construction of a large-scale methanol production plant. Therefore, priority has been given to large sawmills. The distribution of sawmills across the Swedish territory is shown in Figure 5-1. The production capacity of each sawmill is assumed constant over the whole planning horizon.

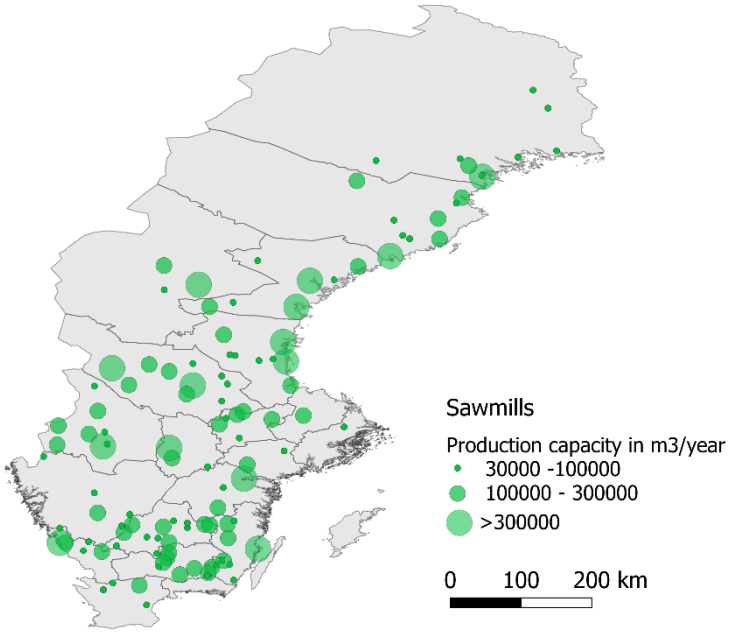

Figure 5-1 *Geographical position and classification per annual production capacity of Swedish sawmills*

The operation characteristics of a sawmill must be understood, so to assess the availability of raw materials that can be destined to methanol production. Sawmills convert harvested logs devoid of branches, roots and treetop into boards called lumbers by following few steps: debarking, sawing, sorting and drying. In some occasions, lumbers can undergo a grinding treatment to enhance the quality of the final product. During the debarking and sawing phases, a substantial part of the raw material is lost to by-products, which other than barks include wood chips and sawdust. In a typical Swedish sawmill, only 47% of the incoming timber is converted into the desired final product, as displayed in Figure 5-2 [61].

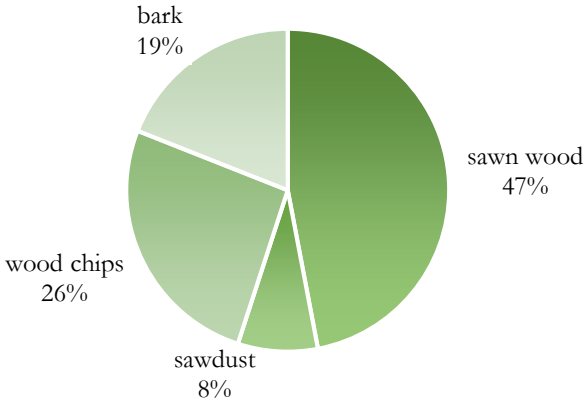

Figure 5-2 *Material balance of typical Swedish sawmill (%weight, dry) [61]*

Typically, the water content in the sawn wood is reduced from an initial level of 50-60% moisture to the desired final value of 18% [62], which makes drying the most energy demanding phase of the sawmilling process [63]. To provide this required energy, a portion of the generated sawmill by-product is burnt on site in a biomass furnace. Bark is the main component of this biomass fuel mix, smaller quantities of sawdust and wood chips are added to facilitate the combustion process [63]. Considering the total internal heat energy demand of a sawmill, which includes room heating and lumber drying, the residues of wood chips and sawdust reduces respectively by 0.6% and 1.1% compared to the value shown in Figure 5-2 [61].

To define the maximum available quantity of feedstock material, the annual production capacity of each sawmill is converted from volume to mass basis, using as bulk density the value obtained through the following relation (Briggs [64]):

$$\rho_{sawn\ wood} = \rho_b \frac{1+M}{1-s} \tag{5.1}$$

where:

- $\rho_{\text{sawn wood}}$ is the density of the sawn wood in kg/m^3;
- ρ_b is the wood basic density, defined as the ratio between the oven dry wood fiber and the volume of fresh wood [62]. The average basic density of coniferous wood used in Swedish sawmills is 415 kg$_{dry}$/m$^3_{fresh}$ [62];
- M is the mass fraction of moisture in the produced sawn wood;
- s is the shrinkage, a volumetric loss induced by the drying process. The average shrinkage loss observed in Swedish sawmills processing coniferous wood has been reported equal to 5% [62].

Then, the feedstock material available at each sawmill can be found by combining the annual production of sawn wood with the conversion factors derived from the sawmill's material balance:

$$m_{wood\ chips\ i} = V_i\ \rho_{sawn\ wood}\ (1-M)\ \frac{f_{wood\ chips} - q_{wood\ chips}}{f_{sawn\ wood}} \tag{5.2}$$

$$m_{sawdust\ i} = V_i\ \rho_{sawn\ wood}\ (1-M)\ \frac{f_{sawdust} - q_{sawdust}}{f_{sawn\ wood}} \tag{5.3}$$

where:

- i represents the i-esim sawmill;
- m is the total available mass of the indicated residue in kg$_{dry}$/year;

- V is the annual sawmill production capacity in m^3/year;
- f is the conversion factor from input log to the specified product;
- q is the internal use for heating purposes of the considered residue material as percentage of the input material.

The feedstock availability can be expressed in energy terms:

$$\bar{b}_i = \left(m_{wood\ chips} + m_{sawdust}\right) \frac{LHV_{wood}}{10^6} \tag{5.4}$$

where:

- $\bar{b}_i$ is the energy content of the available feedstock in TJ/year;
- LHV_{wood} is the energy content of wood in MJ/kg_{dry}.

The residual wood chips and sawdust that are not used for on-site heating purposes already represent an additional source of income for the sawmill. The latter are usually sold to pulp and paper mills, while the former is sold to plants that produce pellets used for heat and electricity generation [63]. Therefore, wood chips and sawdust have a market price, which is included as feedstock cost in the analysis. The price variation of wood chips and sawdust in the Swedish market is shown in Figure 5-3.

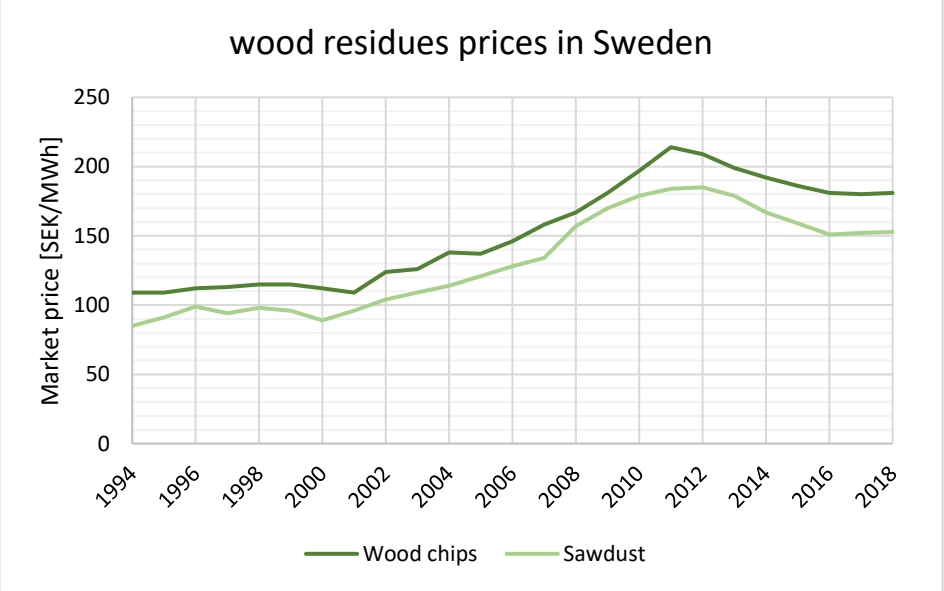

Figure 5-3 *Historical prices for wood chips and sawdust in Sweden [13]*

It can be noticed that the variation trend is similar for the two products over the whole observed timespan, showing a peak in 2011 followed by a steady drop that ended in 2016. The sharp prices rise reported during the 2000s is consequence of the increased demand of wood fuels for electricity and heat generation, which enhanced the competition among different stakeholders interested in cheap wood products [65]. Despite prices of wood residues seem to have recently set on a stable level, a similar situation as observed between years 2000 and 2011 might repeat with the introduction of new stakeholders, as would be the methanol producers described in this study. For this reason, a steady increase of 0.5% per year on the price of wood chips and sawdust is assumed for the rest of the simulation period.

5.2 Costs of methanol production plant

The investment cost per unit capacity of building a methanol synthesis plant is strongly influenced by scaling effects: increasing the size of the plant leads to a lower unit cost [66]. Thus, the choice of the plant size will eventually influence the unit cost of methanol production, so the total plant investment cost is added to the optimization model.
The cost of the methanol plant is obtained with a bottom-up approach, individuating the cost of the main plant components and their scaling factor. A summary of the findings is reported in Table 5-1. Then, the cost of individual components is adjusted by applying the scaling function defined in equation (5.5).

$$\frac{Cost_a}{Cost_b} = \left(\frac{Size_a}{Size_b}\right)^R \tag{5.5}$$

Table 5-1 *Scaling factors and cost of plant components referred to a 380 MW_{th} (LHV_{dry} biomass input) methanol synthesis plant [66], [67], [68]*

Plant system	**Scaling factor (R)**	**Cost [M€]**
Biomass handling and pre-treatment	0.79	22.5
Gasifier (indirect BCL)	0.65	25
Gas cleaning		
Tar cracker	0.7	7.6
Cyclones	0.7	5.6
Heat exchanger	0.6	9.2
Baghouse Filter	0.65	3.2
Condensing Scrubber	0.7	5.6
Syngas Processing		
Compressor	0.85	13.9
Steam Reformer	0.6	37.8
WGS	0.67	1.9
Rectisol™	0.63	16.4
Methanol production		
Make up compressor	0.7	14.3
Gas phase methanol	0.72	9.8
Recycle compressor	0.7	7.2
Refining	0.7	19.5

The process plant cost (PPC) for a selected plant size results from the sum of the adjusted cost of the individual plant components. For the base case 380 MW_{th} methanol synthesis plant, the PPC is 199.54 M€. To the cost of the main plant components, the investment costs reported in Table 5-2 are added to obtain the total plant cost (TPC).

Table 5-2 *Other considered investment costs [66],[69]*

Start-up cost	5% of PPC
Engineering fee	10% of PPC
Process contingency	2.345% of PPC

General plant facilities	10% of PPC
Project contingency	15% of (PPC + general plant facilities)
Land cost	0.8% of PPC

The O&M costs, which includes labour, scheduled maintenance, routine replacement of components and equipment and disposal of residual streams, is assumed to be constant for every year of operation and equal to 4% of the total plant investment cost [70].

Other variable operation costs, as feedstock materials and cost of consumed energy, are also included in the optimization model, even though their unit cost is assumed constant and not dependent on the size of the plant. These costs will be included to determine the total cost of methanol production. Please refer to section 5.1 for assumptions on feedstock material cost and to section 4 for the energy requirements of the methanol synthesis plant.

5.3 Marine transport fuel demand

The historical data about the energy demand for international and domestic marine transport registered in Sweden, displayed in Figure 5-4, have been analysed to obtain a projection of the final energy demand over the considered timespan.

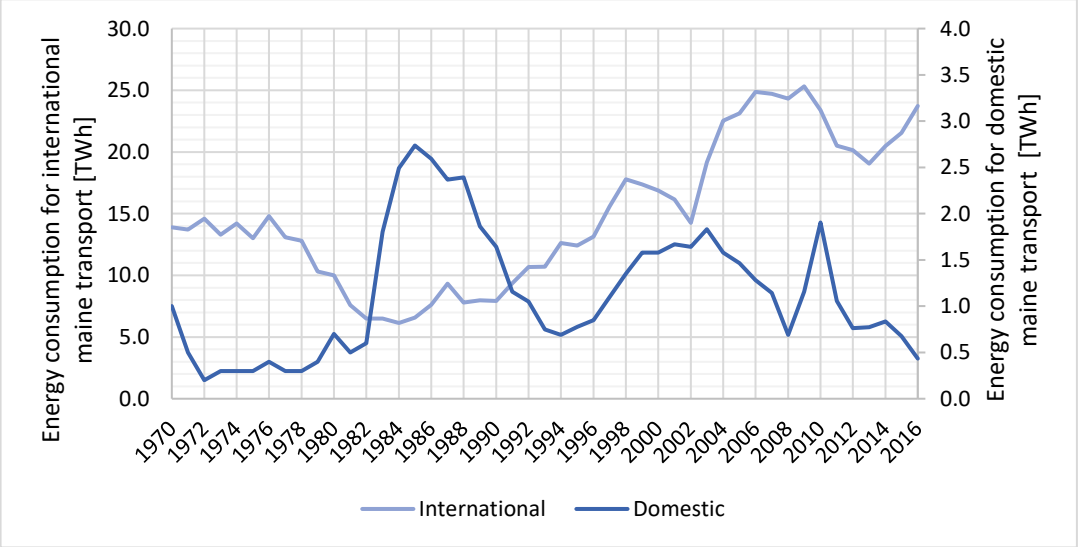

Figure 5-4 *Final energy use for international (left axis) and domestic transport (right axis) in Sweden from 1976 [13]*

Despite some period of regression, the energy consumption for international marine transport shows an overall growing trend. The final energy demand has been rapidly increasing in the recent years, returning almost to the level reached prior the global financial crisis of 2008. Considering this energy demand mainly related to the shipping of goods, it is assumed that the growing trend will continue given the healthy economic conditions of Sweden. A linear interpolation of the available data returns a projected energy demand of 27.7 TWh for 2035, as shown in Figure 5-5.

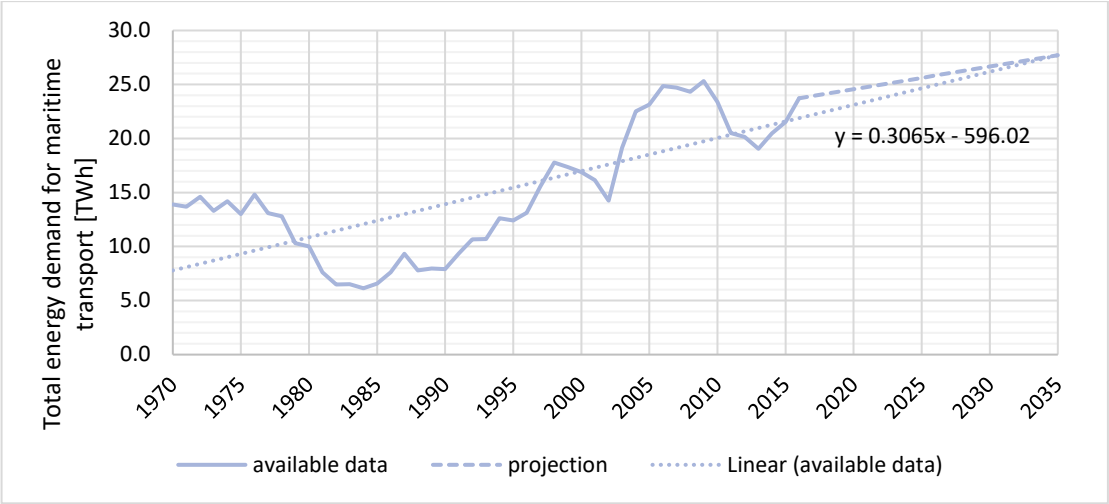

Figure 5-5 *Projected final demand for international marine transport*

On the other hand, the annual energy demand for domestic shipping has been experiencing a steady decline in the recent years, reaching in 2016 the lowest level recorded in the past 35 years. The final energy consumption for domestic marine transport is assumed to remain constant and equal to the value registered in 2016, i.e., 0.43 TWh.

The national energy consumption is then partitioned among the principal ports in Sweden, considering the gross cargo weight loaded at each port on departing vessels. Transportföretagen, the Swedish confederation of transport enterprises, provides information concerning the loaded cargo for both international and domestic marine transport [71]. The list of the identified Swedish ports is reported in Appendix , including geographical locations and cargo data. According to the geographical boundaries selected for the model, only the ports on the mainland are considered. Equation (5.6) defines the energy demand of a single port j.

$$D_j = D_{int}\frac{l_{int_j}}{\sum_{j=1}^{P} l_{int_j}} + D_{dom}\frac{l_{dom_j}}{\sum_{j=1}^{P} l_{dom_j}} \tag{5.6}$$

where:

- j represents the j-esim port;
- P is the total number of ports;
- D is the final energy demand allocated to the port;
- D_{int} and D_{dom} are respectively the international and the domestic marine demand for a considered year;
- l_{int} and l_{dom} are the gross weight of cargo for international and domestic shipping in 2016;

Figure 5-6 shows the geographical location of the considered ports, which are represented with markers of different size, according to the energy demand registered in 2016.

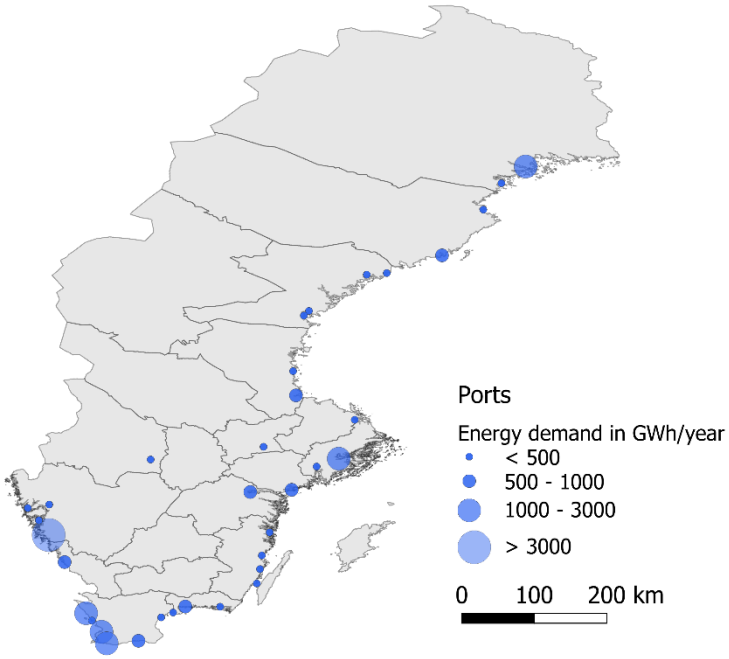

Figure 5-6 *Geographic position of Swedish ports and classification per annual energy demand (in GWh)*

5.4 Optimization model

A MILP model is developed to solve the Facility Location Problem. The problem solution defines the optimum location and the size of the methanol synthesis plants that minimize the total cost of the methanol production chain. This cost comprises of the purchase cost of woodchips and sawdust, the cost for transporting the feedstock from a sawmill to the production plant, the investment cost required for building the plant, the O&M costs of the biomethanol plant and the cost for delivering the final product from the production site to the port.

Fixing the possible sizes of the methanol synthesis plants to $Q = \{100; 200; 300; 400\}$, the following sets are defined:

- $\tilde{S} = \{1, \dots, S\}$, where S is the number of sawmills[1] included in the study;
- $\tilde{P} = \{1, \dots, P\}$, where P is the number of considered ports;
- $\tilde{N} = \{1, \dots, N\}$, where N is the number of considered plant sizes;
- $\tilde{Y} = \{1, \dots, Y\}$, where Y is the number of years in the projected timespan.

The continuous non-negative variables in the model are:

- $b_{i,k,y}$ as the biomass supplied from sawmill i to plant k in year y, measured in TJ;
- $x_{k,j,y}$ as the methanol produced in plant k and delivered to port j in year y, measured in TJ.

Lastly, the binary variable $u_{k,z,y}$ defines if plant k of size z is in operation in year y.
The biomass supplied by each sawmill is limited by the constraint defined in equation (5.7), which considers the maximum amount of biomass available at the sawmill ($\bar{b}_i$) calculated as described by equation (5.4).

[1] sawmills represent both biomass suppliers and potential locations for methanol synthesis plant

$$\sum_{k=1}^{S} b_{i,k,y} \leq \bar{b}_i, \quad i \in \tilde{S}, y \in \tilde{Y} \tag{5.7}$$

Let c_{w_y} and c_{s_y} be respectively the cost of wood chips the cost of sawdust in year *y*. It is assumed that the biomass delivered is a fixed mix of wood chips and sawdust, with the first making up for 78.6%[1] of the energy share. The biomass delivery cost from sawmill *i* to plant *k* in year *y* is obtained as follow:

$$t_{b_{i,k}} = 320 + 9.7\ x\ d_{i,k} \ \text{[72]} \tag{5.8}$$

where:

- $t_{b_{i,k}}$ is the cost of delivering biomass by truck from sawmill *i* to plant *k*, measured in €/$TJ_{biomass}$;
- $d_{i,k}$ is the air distance between sawmill *i* and plant *k* increased by a correction factor of 1.4.

The production of methanol is controlled by constraint (5.9), which limits the production to the energy demand of port *j* in year *y* ($D_{i,y}$ as defined in equation (5.6)).

$$\sum_{k=1}^{S} x_{k,j,y} = s\ D_{j,y}, \quad j \in \tilde{P}, y \in \tilde{Y} \tag{5.9}$$

where *s* is the share of energy demand covered by methanol, set according to the considered scenario.

The methanol is delivered by truck from plant *k* to port *j* at a cost $t_{m_{k,j}}$.

$$t_{m_{k,j}} = 138 + 3.05\ x\ d_{k,j} \ \text{[73]} \tag{5.10}$$

where the transport cost is expressed in €/TJ_{MeOH} and $d_{i,k}$ is the air distance between plant *k* and port *j* increased by a correction factor of 1.4.

The methanol synthesis plant is modelled through an energy balance equation, which includes the biomass-to-methanol conversion efficiency of the plant (η_k).

$$\eta_k \sum_{i=1}^{S} b_{i,k,y} = \sum_{j=1}^{P} x_{k,j,y}, \quad k \in \tilde{S}, y \in \tilde{Y} \tag{5.11}$$

The plant is assigned a size according to the received amount of biomass:

$$\sum_{z=1}^{N} u_{k,z,y}\ h\ Q_z \geq \sum_{i=1}^{S} b_{i,k,y}, \quad z \in \tilde{N}, k \in \tilde{S}, y \in \tilde{Y} \tag{5.12}$$

where h indicates the plant operating hours during a year.
The cost for building a plant of size *z* is I_z and the cost of operation is O_z.

[1] from sawmill material balance: available wood chips = 25.4%, available sawdust = 6.9%; $\frac{25.4}{25.4+6.9} = 78.6$

Equation (5.13) is introduced to limit the chosen size to no more than one of the available options.

$$\sum_{z=1}^{N} u_{k,z,y} \leq 1, \quad k \in \tilde{S}, y \in \tilde{Y} \tag{5.13}$$

Lastly, constraint (5.14) maintains the size of the plant constant after the plant is built.

$$u_{k,z,y} \geq u_{k,z,y-1}, \quad z \in \tilde{N}, k \in \tilde{S}, y \in \tilde{Y} \tag{5.14}$$

For the mentioned costs, the objective function is so defined:

$$\begin{aligned} f(b,x,u) = & \sum_{y=1}^{Y}\sum_{i=1}^{S}\sum_{k=1}^{S} b_{i,k,y}\,(t_{b_{i,k}} + 0.786\,c_{w_y} + 0.214\,c_{s_y}) \\ & + \sum_{y=1}^{Y}\sum_{k=1}^{S}\sum_{j=1}^{P} x_{k,j,y}\,(O_z + t_{m_{k,j}}) \\ & + \sum_{y=1}^{Y}\sum_{k=1}^{S}\sum_{z=1}^{N} Q_z\, I_z(u_{k,z,y} - u_{k,z,y-1}) \end{aligned} \tag{5.15}$$

The Facility Location Problem is defined as

$$\begin{cases} \min\limits_{b,x,u} f(b,x,u) \\ s.t. \\ (5.7), (5.9), (5.11) - (5.15) \\ b_{i,k,y}, x_{k,j,y} \geq 0, \quad i \in \tilde{S}, k \in \tilde{S}, j \in \tilde{P}, y \in \tilde{Y} \\ u_{k,z,y} \in \{0;1\}, \quad k \in \tilde{S}, z \in \tilde{N}, y \in \tilde{Y} \end{cases} \tag{5.16}$$

The described Facility Location Problem is a standard MILP problem, and it is solved in GAMS using the CPLEX algorithm. Once a solution is obtained, the total production cost and the total amount of methanol produced are used to calculate the LCOE of bio-methanol. Let I_y and O_y be the investment cost for building and operating the bio-methanol plants in year y respectively. Then, let F_y be the cost of the necessary feedstock to produce the amount of methanol M_y required during year y. The LCOE of bio-methanol production is defined as in (5.17).

$$LCOE_{bioMeOH} = \frac{\sum_{y=1}^{Y} \frac{I_y + O_y + F_y}{(1+r)^y}}{\sum_{y=1}^{Y} \frac{M_y}{(1+r)^y}} \tag{5.17}$$

This study assumes a discount rate r of 2% and considers 20 years lifetime Y. The LOCE is selected as it considers the net present value of all the costs sustained during the lifetime of the plant, while at the same time it accounts for all the produced methanol. Therefore, the obtained indicator provides a reference value for the methanol production cost that can be compared with the cost related to different technologies, even when involving unequal time

spans or different investment conditions. Moreover, expressing the cost of bio-methanol as LCOE gives a more immediate term of comparison that the total cost of production related to 20 year of plant operation. In this study, the LCOE of bio-methanol is compared to the European market price of the marine fuels currently available in the Baltic area, which are reported in Table 5-3.

Table 5-3 *European market price for marine fuels used in the Baltic sea [74], [75],[76]*

Fuel	Price on the European market [€/MWh$_{fuel}$]
IFO380	29.4
MGO	44.1
LNG	25.2
Methanol[1]	65.8
ULSFO	42.7

5.5 Summary of model assumptions

The following list reports the main assumptions included in the optimization model.

- The system's boundary extends from the sawmill until distribution to port, including feedstock purchase and distribution costs.
- The boundary of Sweden's mainland is considered the geographical boundary of the system.
- The model minimizes the total cost of production, which includes the cost of biomass, the feedstock delivery cost, the plant investment cost, the plant O&M cost and the methanol delivery cost.
- The available feedstock consists of sawdust and woodchips that remain after the sawmilling process.
- Only Swedish sawmills having a production capacity greater than 30000 m^3/year are included in the model as potential suppliers and possible location for the new methanol plant.
- Possible supply of feedstock from outside the system's geographical boundary is neglected.
- All the woodchips and sawdust remaining after the sawmilling process are considered available for methanol production, neglecting the interest of other industries in these products.
- Potential bio-methanol plant is located at the existing sawmill.
- Only one methanol plant can be installed at each sawmill, the new plant has a rated biomass input capacity of either 100, 200, 300 or 400 MW.
- Once the plant is built, the size must remain constant.
- The conversion efficiency of the plant, estimated from energy modelling in Aspen Plus, is 27.4% [69], and the plant operates for 8000 h/year.
- The feedstock cost is assumed according to the Swedish market price of the considered products.
- The transport cost of biomass and methanol neglects the cost of the return trip.
- Only road freight transport is the considered for material transport.
- Both international and domestic energy demands for Swedish maritime transport are considered.

[1] produced from natural gas

- The methanol production completely fulfils the considered fraction of the marine energy demand.

6 Method for estimating the GHG emission reduction potential

This study only considers the environmental impact of GHG emissions related to the direct combustion of the fuel on board of the vessel, referred as tank-to-propeller emissions. The emissions of GHG are expressed in CO_2 equivalent (CO_2eq) emissions, considering the emitted quantities of CO_2, CH_4 and NO_2.

According to the guidelines released in 1991 by the Organization for Economic Cooperation and Development (OECD) in matters of estimating national GHG emissions, ”CO2 emissions resulting from bioenergy consumption should not be included in a country’s official emission inventory” [77]. This convention allows to neglect the contribution of direct emissions of CO_2 when coming from the exploitation of bioenergy sources. Furthermore, the combustion of methanol does not produce any CH_4 or N_2O [15]. For these reasons, the bio-methanol GHG emission factor (EF) is assumed equal to zero in this study. Table 6-1 reports the tank-to-propeller CO_2 emission factors related to the maritime fuels currently used in Sweden, which were obtained after literature review.

Table 6-1 *Tank-to-propeller GHG emission factors for principal maritime fuels used in the Baltic sea [15]*

Fuel	**GHG EF [t_{CO2eq} /MWh_{fuel}]**
IFO380	280.44
MGO	266.04
LNG	217.8
Methanol[1]	248.4
ULSFO	280.44

Bio-methanol is assumed to cover a fixed share s of the Swedish energy demand for maritime transport, replacing the fuels indicated above. Therefore, the consequent amount of saved CO_2 emission for replacing fuel f is calculated as defined in (6.1).

$$saved\ GHG\ emissions_f = s\ x \sum_{j=1}^{P} \sum_{y=1}^{Y} D_{j,y}\ x\ EF_f \qquad (6.1)$$

Where P and Y are the considered number of ports and years in the simulation respectively, and $D_{j,y}$ is the energy demand of port j in year y.

The GHG emissions reduction resulting from replacing the fuels indicated in Table 6-1 with bio-methanol is compared with the total emissions from the Swedish transport sector recorded in 2016, which amounted to 0.013 Gton/CO_2eq [78].

[1] produced from natural gas

7 Scenario development

This thesis evaluates the potential of producing bio-methanol in Sweden to cover the demand for domestic and international marine transport. The opportunity is investigated under two scenarios:

- M5, considers a low fraction of bio-methanol to be blended with FO or MGO. The mixture is burnt in existing conventional CI engines, without the need of retrofitting. This scenario simulates the recently adopted legislation that imposes a minimum fraction of renewable fuels in gasoline and diesel used for road transport purposes. The methanol volumetric fraction is limited to 10% (around 5% on energy basis), to avoid phase separation problems in the mixture.
- M25, aims to satisfy 25% of the Swedish maritime final energy demand with bio-methanol, assuming some of the vessels will be retrofitted to DF operation, so to make feasible the operation with high shares of methanol in the fuel mix.

Therefore, the solution of scenarios M5 provides the total cost for producing the amount of methanol required to cover 5% of Sweden's energy demand for international and domestic maritime transport for each year of the simulation. Whereas, solving scenario M25 delivers the total production cost when the methanol production equals to 25% of the energy demand. After obtaining the solution of the base scenarios, two sensitivity analysis are performed to observe the response of the model results in terms of total production cost, LCOE and optimal location of the plants.

First, constraint is added to the optimization model to limit the maximum transport distance of methanol. The air distance between the methanol plant and the port is reduced respectively to 100 km, 200 km, 300 km and 400 km. This constraint should prevent long travel by road transport, which is the only transport mean considered in this study.

Then, the originally assumed plant's efficiency is gradually increased to observe if some changes are induced to the plants positioning obtained from the base scenarios. An increase of the plant efficiency is expected to diminish the quantity of needed biomass, which directly determines a reduction of the production cost. Moreover, a better plant efficiency could eventually lead to the reduction of the installed plant capacity and even to a different positioning of the production facilities. The initial efficiency value of 27.4% is increased by 10%, 20%, 30%, 40% and 50%.

8 Results and discussions

This chapter presents and discusses the research findings. First, it summarizes the results from the methanol plant model developed in Aspen Plus. Then, the optimization model's outputs are presented for the base blending scenarios, i.e., M5 and M25. Lastly, this section presents the results of the sensitivity analysis.

The model solution provides the locations and the size of the methanol plants that minimize the total production cost of bio-methanol. The total production cost includes the purchase cost of feedstock, the cost for transporting biomass, the capital investment for building the plant, the plant's O&M costs and the cost for delivering bio-methanol to the ports. Moreover, along with the plant location, the model solution includes the feedstock and methanol material streams between each plant and the respective feedstock suppliers and ports. The results confirm that the production of bio-methanol satisfies the energy demand assumed in each scenario, which means that there is an adequate quantity of feedstock within the system boundaries.

8.1 Methanol plant's model results

The results are presented according to 1 MW thermal input of wet biomass. The biomass flow rate is 378.95 kg/h based on dried biomass' LHV of 19 MJ/kg. The simulation returns a pure methanol production of 50.16 kg/h, which represents a biomass-to-methanol conversion efficiency of 27.4%. Moreover, the findings indicate an overall negative heat balance of 213.47 kW over all the heat exchangers and reactors included in the model. According to the adopted sign convention, the result suggests that the system does not require any addition of heat from an external source. Therefore, since process integration is not an objective of this study, the cost of hot utilities is assumed equal to zero. Also, the costs of cold utilities are neglected. Table 8-1 reports the calculated net electrical work required by the blocks included in the model.

Table 8-1 *Obtained electric power consumption of bio-methanol synthesis plant*

Block	Electrical power consumption [kW]
C-DRY	11.71
C-COMB	0.27
C-S1	2.15
C-S2	44.63
PUMP-R	0.03
PUMP-WGS	0.02
C-S3	0.39
C-M1	10.46
C-M2	0.17
C-M3	0.08

The output shows that the electricity cost for operating the plant equals to 28925 €/year, assuming the cost for electricity of 51.6 €/MWh as described in section 4.

The presented plant's efficiency and electricity cost are included in the GAMS optimization model. The former describes the methanol plant by defining the energy balance between the

input material and the final product. Th latter is included as part of the O&M cost for operating the plant.

8.2 Optimal methanol plant's sizes and locations

Several previous studies have investigated the optimization of the biomass supply chain for producing biofuels in biorefineries. In [79], it was concluded that the geographic location of biofuel production facilities should be chosen strategically to minimise the total cost of using the biofuel, and that the favourability of centralized or decentralized configurations of the supply chain is dependent on specific site conditions. Figure 8-1 shows the optimal location of methanol plants found for M5 and M25 scenarios.

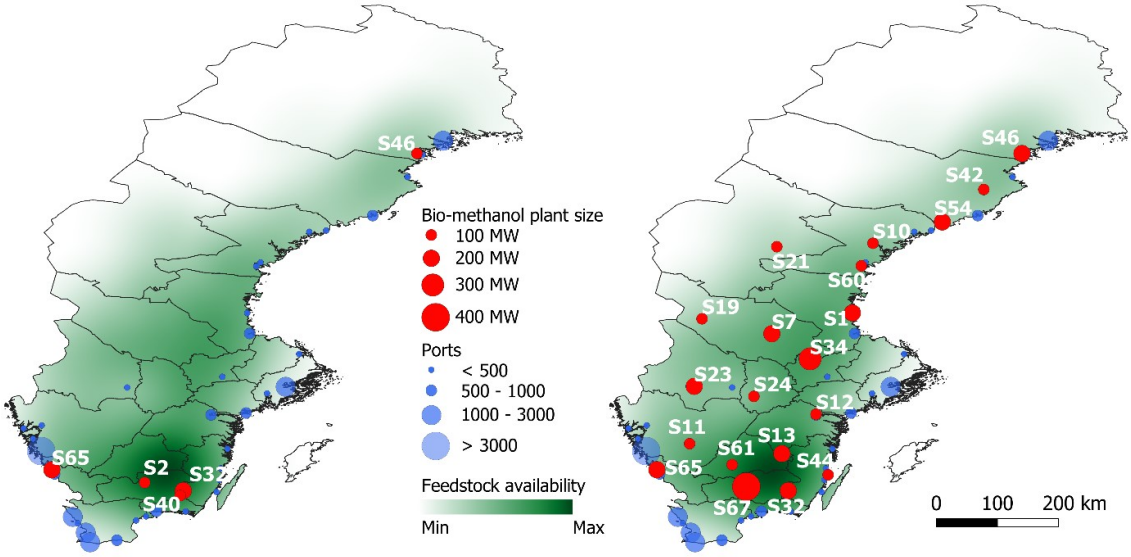

Figure 8-1 *Optimal locations of methanol production plants for scenarios M5 (left) and M25 (right)*

The bio-methanol plants, which were all built in the first year, tend to concentrate in areas with higher availability of feedstock. The trend is particularly evident for scenario M5, where only one plant is positioned in the north of Sweden and all the remaining are placed in the southern territory. Therefore, the central part of the country remains without any production site, despite the presence of a significant number of ports, including those in the Stockholm area. The characteristics of the identified methanol plants are shown in Table 8-2 and

Table **8-3**.

Table 8-2 *Characteristics of methanol plants for M5 scenario*

Methanol plant	Plant size [MW]	Processed biomass [t_{wet}/hour]	Average plant load [%]	Maximum distance between methanol plant and sawmill [km]	Methanol production [kt/year]	Maximum distance between methanol plant and port [km]
S2	100	37.89	100	12.8	40.06	271.1
S32	200	45.46	60.0	66.4	48.06	456.9
S40	100	37.64	99.3	38.8	39.79	195.3
S46	100	37.60	99.2	30.8	39.74	554.8
S65	200	67.06	88.5	75.6	70.89	55.3

Table 8-3 Characteristics of methanol plants for M25 scenario

Methanol plant	Plant size [MW]	Processed biomass [t_{wet}/hour]	Average plant load [%]	Maximum distance between methanol plant and sawmill [km]	Methanol production [kt/year]	Maximum distance between methanol plant and port [km]
S1	200	74.02	97.7	98.0	78.24	284.0
S7	200	73.67	97.2	77.0	77.87	380.0
S10	100	37.89	100	0	40.06	670.1
S11	100	37.89	100	183.7	40.06	69.0
S12	100	37.89	100	85.0	40.06	387.6
S13	200	72.65	95.9	156.7	76.79	286.1
S19	100	37.89	100	48.7	40.06	384.1
S21	100	34.61	91.3	55.1	36.58	608.6
S23	200	75.23	99.3	148.2	79.53	197.1
S24	100	37.89	100	25.2	40.06	223.3
S32	200	75.79	100	75.0	80.11	175.4
S34	300	92.65	81.5	106.5	97.93	490.6
S42	100	32.03	84.5	125.7	33.85	112.0
S44	100	37.26	98.3	47.6	39.38	119.3
S46	200	69.92	92.3	115.5	73.91	47.7
S54	200	51.01	67.3	187.9	53.92	473.4
S60	100	36.87	97.3	72.7	38.97	607.6
S61	100	37.89	100	53.0	40.06	203.4
S65	200	73.56	97.1	91.8	77.76	138.0
S67	400	101.69	67.1	106.1	107.49	177.6

The findings reveal that, for the investigated supply chain, smaller plant sizes (i.e., 100 and 200 MW) are preferred when the objective function is to minimize the total cost of production. This demonstrates that limiting the transport distance of biomass, and with it the cost for transporting the biomass, has a greater impact on reducing the final cost of production than economies of scale that derive from building plants with larger production capacity.

The findings also reveal that the maximum transport distances for delivering methanol from the producing plant to the ports tend to be greater than the largest distance covered by the biomass to reach the production plant. Similar results are observed in both scenarios. Considering all the installed plants, the average distance to transport methanol in scenario M25 equals to 200.5 km, with maximum distance of 670.1 km for part of the methanol transported from plant S10. On the other hand, in the same scenario biomass is received by the plants within an average air distance of 50.6 km. This transport distance reduces to 24.2 km in scenario M5, while the average air distance to transport methanol equals to 204.5 km, similar to scenario M25. The results can be attributed to the combination of two factors. Firstly, in terms of energy unit of the transported product, the biomass transport is more expensive than methanol transport. Secondly, the feedstock material is transported in larger quantity than the final product. The quantity of transported biomass is nearly four times greater than the amount of delivered methanol. Therefore, locating the production sites near the sources of feedstock has primary importance for to the reduction of the total production cost. This explains why the production plants tend to be positioned far away from the end-users, as showed in Figure 8-1. Moreover, this behaviour directly results in very large delivery distances of the final product, which are not considered realistic for the selected transportation mean. For this reason, the described optimization model is implemented with a constraint that limits the maximum air distance between a production site and the receiving ports. The influence of the new constraint on the model's base results is presented in section 8.5.

The results indicate that only few plants operate at full capacity for the entire timespan. Particularly low values are observed for plant S32 in M5 scenario and for plants S54 and S67 for M25 scenario. Considering the whole simulation time, the aforementioned plants receive biomass for less than 70% of the rated capacity. The rest of the methanol plants operates above 90% of the rated capacity. However, in the final year of the simulation only one bio-methanol plant per scenario does not operate at full capacity. Plant S32 in scenario M5 and plant S67 in M25 receive biomass for 70% and 76% of the rated input capacity respectively during the last year. This is considered a direct consequence of the limited options defined as possible size for the bio-methanol plant, which makes the production capacity a discrete variable. Therefore, the model forces the choice of one plant larger than the minimum necessary capacity that is needed to fulfil the required demand, to avoid the violation of the methanol production constraint defined by equation (4.9). The remaining bio-methanol plants do not always function at full capacity for two reasons. Constraint (4.14) enforces the plant to maintain the same size throughout the whole planning horizon, making the production capacity of the plant constant. However, the energy demand for maritime transport is assumed to grow steadily, making also the required methanol production increasing from one year to the following. As result, to minimize the total cost of production is required for some plants to operate at partial load during an initial period of the lifetime. Except plants S32 and S67 for scenario M5 and M25 respectively, all the plants operate at the rated production capacity on the last year of the simulation, even though the full capacity working conditions might be reached in different years.

8.3 Total cost

The output of the model provides total production cost of methanol which includes each cost component in the production chain. The results for the M5 and M25 base scenarios are summarized in Table 8-4.

The findings demonstrate that the share of each cost component to the total cost is similar for M5 and M25 scenarios. While the plant's installation and O&M costs show a larger contribution to the total cost in scenario M5 than in M25, the costs related to transporting feedstock and final product present a larger share in scenario M25. In both cases, the feedstock material accounts for almost 50% of the total production cost, suggesting that variations of the cost related to biomass consumption can highly affect the production cost of methanol.

The LCOE of bio-methanol production does not differ significantly in both scenarios. When compared to the market price of the other fuels used in Sweden for maritime transport, the cost of bio-methanol results remarkably high. The study reveals that the estimated bio-methanol cost per unit of energy is more than twice the market price of methanol produced from natural gas and more than five times the price of a conventional IFO.

Table 8-4 *Summary of costs for M5 and M25 base scenarios*

Results	**M5**	**M25**
Methanol demand [PJ]	76.4	382.1
Methanol production [kt]	4770.8	23854.8
Total cost [billion €]	3.29	16.25
$LCOE_{bioMeOH}$ [€/MWh]	148.2	144.2
Cost breakdown [% of total cost]		
Plant investment cost	19.5%	17.7%
Cost of feedstock	47.5%	48.6%
Cost of transporting biomass to the plant	4.3%	6.2%
Cost of plant's O&M	26.7%	24.9%
Cost of transporting methanol to the ports	2.0%	2.6%

8.4 GHG emissions reduction potential

Figure 8-2 shows the amount of avoided GHG emissions from replacing IFO380, MGO, LNG, conventional methanol and ULSFO with bio-methanol. The findings are compared with the total GHG emissions from the Swedish transport sector recorded in 2016.

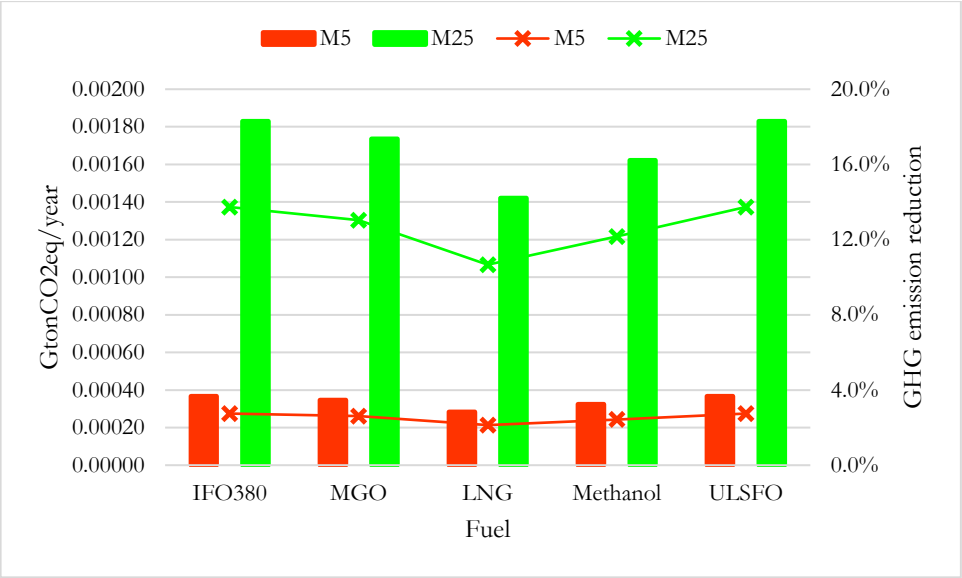

Figure 8-2 *Gross GHG emissions avoided (left axis) and resulting GHG emissions reduction in comparison to 2016 levels (right axis).*

The benefits in terms of GHG emissions reduction are greater when larger quantities of methanol are produced. It can be noticed that the use of methanol derived from natural gas has limited effect towards mitigating the GHG emissions of the maritime transport sector, while bio-methanol guarantees a decrease in emissions up to 13.7% compared to 2016 emissions level.

8.5 Sensitivity analysis on maximum methanol transport distance

The simulation is repeated with new constraint that limits the transport distance of the final product. The maximum air distance between the methanol producer and the receiving port is reduced to 100, 200, 300 and 400 km. The variation of bio-methanol LCOE is displayed in Figure 8-3.

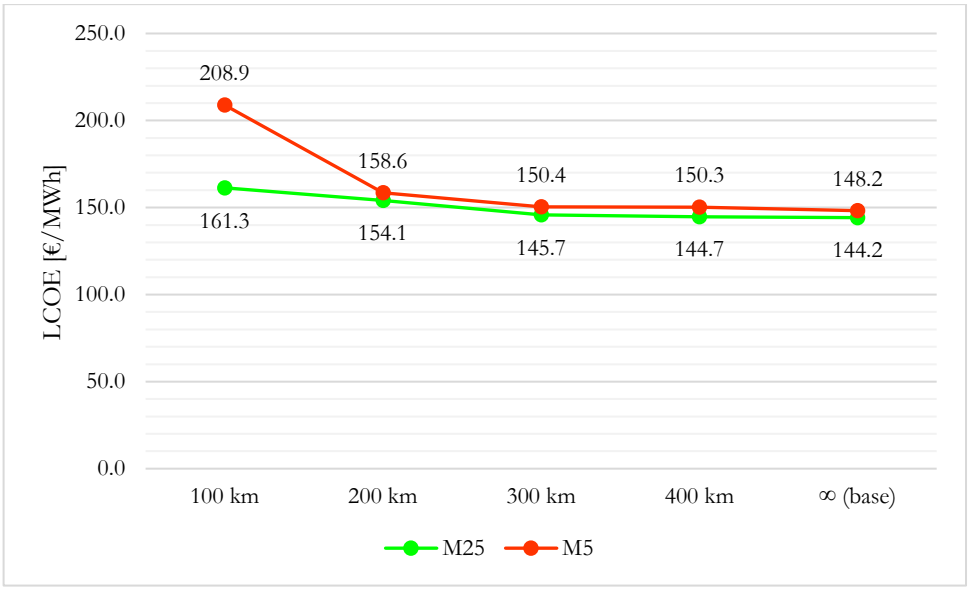

Figure 8-3 *Variation of bio-methanol LCOE as function of the maximum imposed air distance between methanol producer and receiving port*

The findings reveal that the LCOE of methanol tends to decrease for longer methanol maximum transport distances. The variation of the production cost results more significant when the methanol delivery distance is reduced below 300 km. The growth is more evident for scenario M5, where the LCOE reaches 208.9 €/MWh for a maximum delivery air distance of 100 km, increasing by 40.9% compared to the base scenario. The LCOE obtained for scenario M25 shows a more regular rise, containing the variation within 11.9% of the initial value. Figure E-1 and Figure E-2 of Appendix show the optimal methanol plant's locations for scenario M5 and M25 respectively. It is observed that, when the maximum methanol transport distance is reduced, the production sites are positioned closer to the ports. While this reduces the methanol transport cost, it also removes the methanol plants from areas with great availability of feedstock. Consequently, biomass travels for longer distances and the feedstock transport cost rises. Since the feedstock material is transported in larger quantity than the final product and biomass transport is more expensive than methanol transport, the variation of biomass transport cost is generally greater than the reduction of methanol transport cost.

The total cost of methanol production found from each simulation is divided in each cost component, which is compared to the results given by the base scenarios. Considering that the costs of woodchips and sawdust are maintained equal to what assumed in the base scenario, and that the quantity of required biomass is also unchanged, the cost of feedstock is not subjected to any variation within the same scenario. Therefore, the cost of feedstock is omitted from the sensitivity analysis, which findings are presented in Figure 8-4.

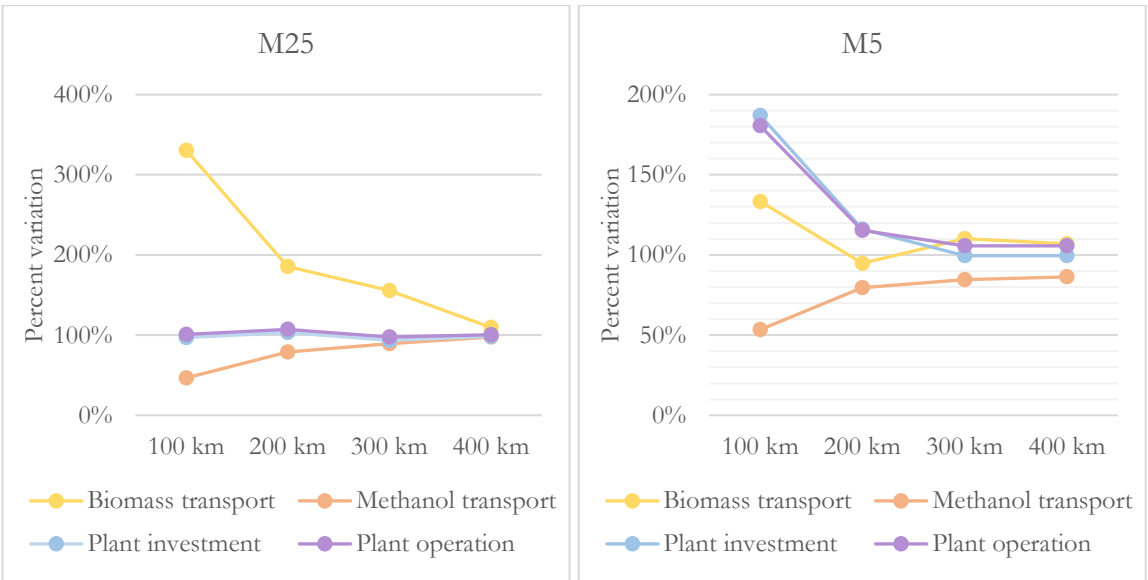

Figure 8-4 *Results of sensitivity analysis on the variation of distance's constraint for methanol transport in percentage compared to the base scenario.*

The findings show slightly different responses between the two assumed scenarios. In both cases, the costs related to the transportation of materials follow the same trend. When the maximum transport distance is increased, the methanol transport cost also increases, due to the imposed reduction of the transporting distance, while the biomass transport cost is generally reducing. This growth results more significant for M25 scenario than for M5, which even registered a cost reduction passing from 300 km to 200 km of maximum methanol delivery distance.

The main difference between the two scenarios concerns the variation of the costs related to plant investment and operation. These costs reduces in scenario M5 for longer methanol transport distance, while in scenario M25 remain almost constant, despite some differences regarding the size distribution of the installed plants, as showed in Figure E-2 of Appendix E. Observing the individuated plant locations for scenario M5, reported in Figure E-1 of Appendix E, it can be noticed that the number of plants increases drastically when the methanol delivery radius is limited to 100 km. In this case, the total capacity of bio-methanol plants equals to 1200 MW, while only 700 MW where installed in the reference scenario. This results in the growth of plant investment and operation costs showed in Figure 8-4. A similar situation is observed for methanol delivery distances lower than 200 km. Despite the greater number of plants, in this case the total installed capacity is 800 MW, resulting slightly higher than in the reference scenario and the same as for 300 km and 400 km delivery radius. However, the presence of a greater number of plants increases the plant investment cost, as result of economies of scale.

In conclusion, the increase of the biomass transportation cost is the only factor that induces the growth of the bio-methanol LCOE for scenario M25. While for scenario M5, the rise of methanol LCOE is a combination of the larger plant investment cost and of the greater biomass transport cost.

8.6 Sensitivity analysis on plant biomass-to-methanol conversion efficiency

This section presents the results obtained from the sensitivity analysis on the plant conversion efficiency, which was increased by 10, 20, 30, 40 and 50% compared to the value assumed in the reference scenarios, e.g. 27.4%. Figure 8-5 displays the variation of the calculated LCOE of bio-methanol for each simulation.

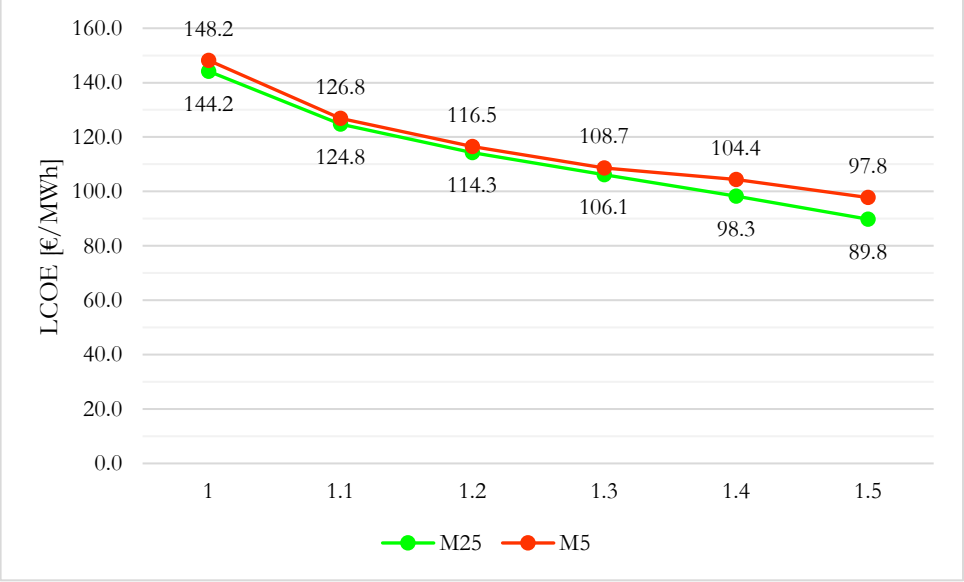

Figure 8-5 *Variation of bio-methanol LCOE as function of the ratio between the new assumed plant efficiency and the value considered in the base scenario*

The findings reveal a steady reduction of bio-methanol LCOE for greater plant efficiencies, showing a maximum decrease of 37.7% and 34.0% for scenario M25 and M5 respectively.

The decreasing trend is similar for both scenarios. However, it is observed that an improvement of plant efficiency between 30% and 50% has a more beneficial effect in scenario M25, increasing the difference of bio-methanol's LCOE between the two scenarios. Figure 8-6 reports the variation of the different cost components in comparison with the base scenario.

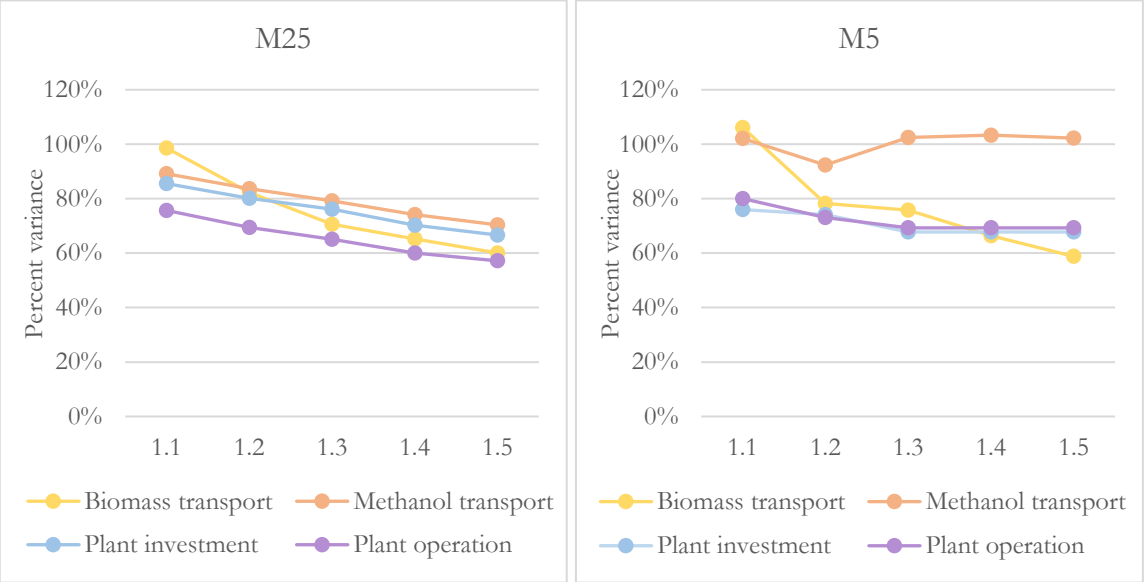

Figure 8-6 *Results of sensitivity analysis on the variation of plant efficiency in percentage compared to the base scenario*

The feedstock purchase cost, which is not displayed in Figure 8-6, is decreasing for each scenario as the efficiency growth results in reducing the quantity of required input material. Figure 8-6 shows that all the cost components are reducing for scenario M25. Particularly, the costs related to plant investment and operation display an almost linear decreasing trend. Table 8-5 reports the number of plants and total installed capacity that is obtained for each simulation.

Table 8-5 *Results from efficiency sensitivity analysis on scenario M25: number of individuated bio-methanol plants and total installed biomass input capacity*

η/η_{base}	Number of plants	Total installed capacity [MW_{th}]
1	20	3300
1.1	15	3000
1.2	15	2700
1.3	15	2500
1.4	14	2300
1.5	13	2200

It is observed that the growth of efficiency results in a constant drop of the installed capacity needed to fulfil the imposed bio-methanol demand. Also, this reduction generally causes the number of installed plants to diminish. The changes in matter of installed capacity and number of plants are accompanied by a variation of the plant distribution across the Swedish territory, as shown in Figure F-2. The different positioning of the plants allows to obtain the constant reduction of the cost related to methanol transportation that is exhibited in Figure 8-6.

The findings related to M5 scenario shows a more irregular behaviour. Despite the cost of transporting biomass is generally diminishing, a 10% increase of efficiency produces a slight increase of 6% for this cost in comparison to the reference scenario. However, Figure F-1 shows that the number of installed plants drops from five to three, resulting in 100 MW decrease of installed capacity that leads to the reduction of plant investment and operation costs. These costs remain unchanged when the efficiency is increased by 30, 40 and 50% because the optimization model returns the same locations and sizes of the bio-methanol plants.

9 Conclusions

This work investigates the potential of methanol production from sawmills residues in Sweden, as possible solution to more sustainable maritime transport. The study considers two blending scenarios, M5 and M25, for partially cover Sweden's energy demand for domestic and international maritime transport. The objective is to determine the minimum cost of methanol production using a MILP model to optimize the supply chain and considering only methanol as valuable product obtained from the biorefinery.

The results from the simulation are consistent for both scenarios. The findings reveal that, in order to minimize the cost of producing bio-methanol from sawmill's by-products, the production facilities must be located next to the source of biomass. Furthermore, this study demonstrates that plants of smaller rated capacity are preferred over larger ones, demonstrating that reducing the distance, hence the cost, of biomass transportation produces a greater benefit towards reducing the production cost than taking advantage of economies of scale related to the construction of larger facilities.

The LCOE of bio-methanol results 148.2 and 144.2 €/MWh for scenario M5 and M25 respectively. The estimated costs are considerably higher than the European market price of the other maritime fuels currently used for maritime transport in the Baltic sea. Particularly, the findings reveal that the bio-methanol LCOEs result twice higher than the current European market price of conventional methanol, which is produced from natural gas. However, this study considers bio-methanol as unique products generated at the biorefinery, neglecting any possible integration between the plant and other industries for utilizing methanol plant's excess heat and by-products. Furthermore, the study does not include any possible economic gain for the reduction of GHG emissions resulting from the use of bio-methanol as fuel for maritime transport. Lower production costs can be reached by investigating possible industry synergies and by applying carbon taxes to the model.

The optimal location of bio-methanol production plants often induces very large distances to cover for transporting the final product to the considered Swedish ports. Limiting the radius of bio-methanol delivery results in a further increase of the bio-methanol LCOE, since the reduction of cost related to transporting the final product is overcome by the growth of the feedstock transport cost. The difference is more evident for scenario M5.

The bio-methanol LCOE results highly sensitive on variation of the assumed biomass-to-methanol conversion efficiency of the plant. The cost of feedstock represents more than 50% of the total production cost. Hence, improving the plant performances directly reduces the quantity of biomass needed by the conversion process and results in a reduction of the production cost. Additionally, the growth of plant efficiency generally diminishes the total installed capacity, causing a drop of the costs related to plant investment and operation. For plant efficiency of 41.1% (based on LHV), the difference between the obtained bio-methanol LCOE and the European market price of conventional methanol reduces by 70% compared to what observed for the reference scenarios.

Lastly, this study demonstrates that introducing bio-methanol in the Swedish maritime fuels market as an alternative to the currently used fuels can potentially have a great impact towards mitigating the GHG emissions from the entire Swedish transportation sector. Considering emissions data related to year 2016, a reduction of GHG emissions from transport applications of 13.7% is observed if 25% of the IFO demand is replaced by bio-methanol.

The GHG emissions reduction drops to 12.2% if bio-methanol is used instead of conventional methanol. The presented results underline that, despite the great difference between the obtained LCOE of bio-methanol and the market price of the conventional maritime fuels, using bio-methanol as maritime fuel is an option worth to be considered when addressing the mitigation of GHG emissions from this sector.

References

[1] UNFCCC, 2015. Decision 1/CP.21 Adoption of the Paris Agreement.
[2] IEA, 2018. Renewables 2018: Analysis and Forecast to 2023.
[3] REN21, 2017. Renewables 2017: Global Status Report.
[4] IEA, 2018. CO2 Emissions from Fuel Combustion Highlights 2018.
[5] EIA, 2016. International Energy Outlook 2016.
[6] European Commission, 2016. Proposal for a directive of the European Parliament and of the Council on the promotion of the use of energy from renewable sources (recast).
[7] Share of transport fuel from renewable energy sources [WWW Document]. Eurostat. URL https://ec.europa.eu/eurostat/web/products-eurostat-news/-/DDN-20180312-1 (accessed 2.13.19).
[8] European Commission - PRESS RELEASES - Press release - A European Strategy for low-emission mobility [WWW Document]. European Commission. URL http://europa.eu/rapid/press-release_MEMO-16-2497_en.htm (accessed 3.18.19).
[9] Transport emissions [WWW Document]. Climate Action - European Commission. URL https://ec.europa.eu/clima/policies/transport_en (accessed 2.13.19).
[10] Regulation (EU) 2018/842 of the European Parliament and of the Council of 30 May 2018 on binding annual greenhouse gas emission reductions by Member States from 2021 to 2030 contributing to climate action to meet commitments under the Paris Agreement and amending Regulation (EU) No 525/2013 (Text with EEA relevance), 2018.
[11] Effort sharing: Member States' emission targets [WWW Document]. Climate Action - European Commission. URL https://ec.europa.eu/clima/policies/effort_en (accessed 2.13.19).
[12] Sweden's integrated national energy and climate plan Draft 2018, 2018.
[13] Swedish Energy Agency, Energy in Sweden – Facts and Figures 2018, available at http://www.energimyndigheten.se/en/news/2018/energy-in-sweden---facts-and-figures-2018-available-now/ (accessed 2.13.19).
[14] Swedish Energy Agency, 2018. Energy in Sweden 2018: An Overview.
[15] Trafikanalys, 2016. Fuels in the Baltic Sea after SECA PM 2016:12.
[16] A. Datta, S. Dutta, B. Mandal, 2014. Effect of Methanol Addition to Diesel on the Performance and Emission Characteristics of a CI Engine.
[17] Norden Energy & Transport, 2014. SPIRETH – End of Project Report Activities and Outcomes of the SPIRETH (Alcohol (Spirits) and Ethers as Marine Fuel) Project.
[18] EA Engineering, Science, and Technology, 1999. Methanol refuelling station costs. Prepared for American methanol foundation.
[19] Forests and Forestry in Sweden [WWW Document]. Royal Swedish Academy of Agriculture and Forestry. URL https://www.skogsstyrelsen.se/globalassets/in-english/forests-and-forestry-in-sweden_2015.pdf
[20] Lim M.K., Ouyang, Y., 2016. Biofuel Supply Chain Network Design and Operations, in: Atasu, A. (Ed.), Environmentally Responsible Supply Chains. Springer International Publishing, Cham, pp. 143–162. https://doi.org/10.1007/978-3-319-30094-8_9
[21] Akgul O., Zamboni A., Bezzo F., Shah N., Papageorgiou L.G., 2011. Optimization-Based Approaches for Bioethanol Supply Chains. Ind. Eng. Chem. Res. 50, 4927–4938. https://doi.org/10.1021/ie101392y
[22] Tursun D.U., Kang S., Onal H., Ouyang Y., Scheffran J., 2008. Optimal Biorefinery Locations and Transportation Network for the Future Biofuels Industry in Illinois, in:

Farm Foundation, Transition to a Bio Economy Conferences, Environmental and Rural Development Impacts Conference, October 15-16, 2008, St. Louis, Missouri. pp. 149–166.
[23] Leduc S., Schwab D., Dotzauer E., Schmid E., Obersteiner M., 2008. Optimal location of wood gasification plants for methanol production with heat recovery. International Journal of Energy Research 32, 1080–1091. https://doi.org/10.1002/er.1446
[24] Gunnarsson H., Rönnqvist M., Lundgren J.T., 2004. Supply chain modelling of forest fuel. European Journal of Operational Research 158, 103–123. https://doi.org/10.1016/S0377-2217(03)00354-0
[25] Leduc S., Lundgren J., Franklin O., Dotzauer E., 2010. Location of a biomass based methanol production plant: a dynamic problem in northern Sweden. Applied Energy 87, 68–75.
[26] IMO, 1997. Protocol of 1997 to amend the International Convention for the Prevention of Pollution from Ships of 2 November 1973, as modified by the Protocol of 17 February 1978.
[27] IMO, 2008. Report of the Marine Environment Protection Committee on its Fifty-Eight Session Attached are annexes 13 and 14 to the report of the Marine Environment Protection Committee on its fifty-eighth session (MEPC 58/23).
[28] European Commission, 2016. D3.1 State-of-the-Art Report Certification, Monitoring and Enforcement.
[29] Månsson S., 2017. Prospects for renewable marine fuels - A multi-criteria decision analysis of alternative fuels for the maritime sector. Department of Energy and Environment Division of Physical Resource Theory Chalmers University of Technology
[30] Methanex Investor Presentation May 2018 [WWW Document]. Methanex. URL https://www.methanex.com/sites/default/files/investor/MEOH%20Presentation%202018-05-16.pdf (accessed 2.18.19).
[31] The Methanol Industry [WWW Document]. Methanol Institute. URL http://www.methanol.org/the-methanol-industry/ (accessed on 2.13.19).
[32] Bertau M., Offermanns H., Plass L., Schmidt F., Wernicke H.-J. (Eds.), 2014. Methanol: The Basic Chemical and Energy Feedstock of the Future. Springer Berlin Heidelberg, Berlin, Heidelberg.
[33] Miller B.G., 2017. 14 - Emerging Technologies for Reduced Carbon Footprint, in: Miller, B.G. (Ed.), Clean Coal Engineering Technology (Second Edition). Butterworth-Heinemann, pp. 669–689.
[34] Renewable energy in Piteå - Business [WWW Document]. Piteå municipality websites. URL https://www.pitea.se/en/Business/Renewable-energy-in-Pitea/ (accessed 2.18.19).
[35] Södra commences biofuel production [WWW Document]. Södra. URL https://www.sodra.com/en/about-sodra/press/press-releases/2658273/ (accessed 2.18.19).
[36] VärmlandsMetanol [WWW Document]. URL http://www.varmlandsmetanol.se/Om%20Projektet.htm (accessed 2.18.19).
[37] World´s first Commercial Scale Biomethanol Plant in Hagfors SWEDEN [WWW Document]. URL http://www.varmlandsmetanol.se/dokument/History_2017.pdf (accessed 2.18.19)
[38] Basu P., 2010. Biomass Gasification and Pyrolysis Practical Design.
[39] Molino A., Chianese S., Musmarra D., 2016. Biomass gasification technology: The state of the art overview. Journal of Energy Chemistry 25, 10–25.

[40] Heyne S., Thunman H., Harvey S., 2013. Exergy-based comparison of indirect and direct biomass gasification technologies within the framework of bio-SNG production. Biomass Conv. Bioref. 3, 337–352.
[41] Woolcock P.J., Brown R.C., 2013. A review of cleaning technologies for biomass-derived syngas. Biomass and Bioenergy 52, 54–84.
[42] Scala F., 2013. Fluidized Bed Technologies for Near-Zero Emission Combustion and Gasification: Woodhead Publishing Series in Energy 59, Woodhead Publishing Series in Energy 1. Woodhead Publishing Ltd.
[43] Devi, L., Ptasinski, K.J., Janssen, F.J.J.G., 2003. A review of the primary measures for tar elimination in biomass gasification processes. Biomass and Bioenergy 24, 125–140.
[44] Milne, T.A., Evans, R.J., Abatzaglou, N., 1998. Biomass Gasifier "'Tars'": Their Nature, Formation, and Conversion.
[45] Spath P.L., Dayton D.C., 2003. Preliminary Screening -- Technical and Economic Assessment of Synthesis Gas to Fuels and Chemicals with Emphasis on the Potential for Biomass-Derived Syngas (No. NREL/TP-510-34929). National Renewable Energy Lab., Golden, CO. (US).
[46] Yao C., Pan W., Yao A., 2017. Methanol fumigation in compression-ignition engines: A critical review of recent academic and technological developments. Fuel 209, 713–732.
[47] Song R., Liu J., Wang L., Liu S., 2008. Performance and Emissions of a Diesel Engine Fuelled with Methanol. Energy & Fuels 22, 3883–3888.
[48] Verhelst S., Turner J.W., Sileghem L., Vancoillie J., 2019. Methanol as a fuel for internal combustion engines. Progress in Energy and Combustion Science 70, 43–88.
[49] Huang Z.H., Lu H.B., Jiang D.M., Zeng K., Liu B., Zhang J.Q., Wang X.B., 2004. Engine performance and emissions of a compression ignition engine operating on the diesel-methanol blends. Proceedings of the Institution of Mechanical Engineers, Part D: Journal of Automobile Engineering 218, 435–447.
[50] Yao C., Cheung C.S., Cheng C., Wang Y., Chan T.L., Lee S.C., 2008. Effect of Diesel/methanol compound combustion on Diesel engine combustion and emissions. Energy Conversion and Management 49, 1696–1704.
[51] Sarvi A., Fogelholm C.-J., Zevenhoven R., 2008. Emissions from large-scale medium-speed diesel engines: 2. Influence of fuel type and operating mode. Fuel Processing Technology 89, 520–527.
[52] Stena Germanica's Methanol Conversion [WWW Document]. StenaLine. URL http://www.stenalinefreight.com/news/Methanol-project (accessed 2.18.19).
[53] Methanol: The marine fuel of the future [WWW Document]. URL http://www.methanol.org/wp-content/uploads/2016/07/Updates-from-Stena-Germanica-Per-Stefenson.pdf (accessed 2.18.19).
[54] Methanol-fueled vessels mark one year of safe, reliable, and efficient operations [WWW Document]. Waterfront Shipping. URL https://www.wfs-cl.com/news/2017/04/methanol-fueled-vessels-mark-one-year-safe-reliable-and-efficient-operations (accessed 2.18.19).
[55] METHANOL - A future fuel for shipping IHS Chemical World Methanol Conference, 12 November 2015 [WWW Document]. Stena AB Group. URL http://www.methanol.org/wp-content/uploads/2016/07/Stena-Methanol-Future-Fuel-Shipping-IHS-World-Methanol-Conference-Nov15.pdf (accessed 2.18.19).
[56] Doherty W., Reynolds A., Kennedy D., 2013. Aspen Plus Simulation of Biomass Gasification in a Steam Blown Dual Fluidised Bed. Book Chapter: Materials and processes

for energy: communicating current research and technological developments, A. Méndez-Vilas (Ed.), Formatex Research Centre.
[57] Prices on electricity for industrial consumers 2007– [WWW Document]. Statistiska Centralbyrån. URL http://www.scb.se/en/finding-statistics/statistics-by-subject-area/energy/price-trends-in-the-energy-sector/energy-prices-on-natural-gas-and-electricity/pong/tables-and-graphs/average-prices-by-half-year-2007/prices-on-electricity-for-industrial-consumers-2007/ (accessed 5.16.19).
[58] Hamelinck C.N., Faaij A., 2001. Future prospects for production of methanol and hydrogen from biomass: system analysis of advanced conversion concepts by ASPEN-plus flowsheet modelling. Utrecht University, Copernicus Institute, Science Technology Society, Utrecht.
[59] Sultana A., Kumar A., 2011. Optimal configuration and combination of multiple lignocellulosic biomass feedstocks delivery to a biorefinery.
[60] Sawmills [WWW Document]. The Sawmill Database. URL https://www.sawmilldatabase.com/sawmills.php?countryid=1&companyid=-1&productionfrom=100000&productionto= (accessed 3.18.19).
[61] Anderson J.-O., Westerlund L., 2011. Surplus biomass through energy efficient kilns. Applied Energy 88, 4848–4853.
[62] UNECE/FAO, 2010. Forest products conversion factors for the UNECE region.
[63] Anderson J.-O., Toffolo A., 2013. Improving energy efficiency of sawmill industrial sites by integration with pellet and CHP plants. Applied Energy 111, 791–800.
[64] Briggs D., 1994. Forest products measurements and conversion factors: With Special Emphasis on the U.S. Pacific Northwest.
[65] Swedish Energy Agency, 2017. Energy in Sweden 2017.
[66] Hamelinck C.N., Faaij A.P.C., 2002. Future prospects for production of methanol and hydrogen from biomass. Universiteit Utrecht Copernicus Institute Department of Science, Technology and Society. Journal of Power Sources 111, 1–22.
[67] Sørensen Å.L., 2005. Economies of Scale in Biomass Gasification Systems.
[68] Holmgren K.M., 2015. Investment cost estimates for gasification-based biofuel production systems.
[69] Leduc, S., Schmid, E., Obersteiner, M., Riahi, K., 2009. Methanol production by gasification using a geographically explicit model. Biomass and Bioenergy 33, 745–751.
[70] IRENA, 2018. Renewable Power Generation Costs in 2017, International Renewable Energy Agency.
[71] Statistical figures – Swedish Ports 2016 and 2015 [WWW Document]. Transportföretagen. URL http://www.transportforetagen.se/In-English/Association-ports-of-Sweden/Statistics/2015-and-2016/ (accessed 3.18.19).
[72] de Jong S., Hoefnagels R., Wetterlund E., Pettersson K., Faaij A., Junginger M., 2017. Cost optimization of biofuel production – The impact of scale, integration, transport and supply chain configurations. Applied Energy 195, 1055–1070.
[73] Börjesson, P., Gustavsson, L., 1996. Regional production and utilization of biomass in Sweden. Energy 21, 747–764.
[74] Rotterdam Bunker Prices [WWW Document]. Ship & Bunker. URL https://shipandbunker.com/prices/emea/nwe/nl-rtm-rotterdam (accessed 5.9.19).
[75] Methanex posts regional contract methanol prices for North America, Europe and Asia. [WWW Document]. Methanex. URL https://www.methanex.com/our-business/pricing (accessed 5.9.19).
[76] European Commission, 2018. Quarterly Report Energy on European Gas Markets - Market Observatory for Energy DG Energy Volume 11 (issue 4, fourth quarter of 2018).

[77] Intergovernmental Panel on Climate Change, Organisation for Economic Co-operation and Development, United States (Eds.), 1991. Estimation of greenhouse gas emissions and sinks: final report from the OECD Experts Meeting, 18-21, February 1991, Rev. Aug. 1991. ed. OECD, Paris, France.
[78] Greenhouse gas emissions increased during all quarters of 2016 [WWW Document]. Statistiska Centralbyrån. URL http://www.scb.se/en/finding-statistics/statistics-by-subject-area/environment/environmental-accounts-and-sustainable-development/system-of-environmental-and-economic-accounts/pong/statistical-news/environmental-accounts--emissions-to-air-q4-2016/ (accessed 5.10.19).
[79] Zetterholm J., Pettersson K., Leduc S., Mesfun S., Lundgren J., Wetterlund E., 2018. Resource efficiency or economy of scale: Biorefinery supply chain configurations for co-gasification of black liquor and pyrolysis liquids. Applied Energy 230, 912–924. https://doi.org/10.1016/j.apenergy.2018.09.018

Appendix 1

Table A-1 *Design specification AIR-DRY*

Variable		**Definition**	
T		Stream-Var Stream=DRIED-W Substream=MIXED Variable=Temp Units=C	
Specification		**Manipulated variable**	
Spec	T	Type	Stream-Var
Target	100	Stream	AIR-IN
Tolerance	0.001	Substream	MIXED
		Variable	MASS-FLOW
Manipulated variable limits		Units	kg/s
Lower	1		
Upper	10		

Table A-2 *Design specification AIR-COMB*

Variable		**Definition**	
CHAR		Mole-Flow Stream=CHAR Substream=MIXED Component=C Units=kmol/hr	
O2		Mole-Flow Stream=AIR Substream=MIXED Component=O2 Units=kmol/hr	
Specification		**Manipulated variable**	
Spec	O2	Type	Stream-Var
Target	1.2*CHAR	Stream	AIR
Tolerance	0.0001	Substream	MIXED
		Variable	MOLE-FLOW
Manipulated variable limits		Units	kmol/hr
Lower	0		
Upper	100		

Table A-3 *Design specification T-COMB*

Variable		**Definition**	
TGAS		Stream-Var Stream=GAS-PROD Substream=MIXED Variable=TEMP Units=C	
TCOMB		Block-Var Block=COMB Variable=TEMP Sentence=PARAM Units=C	
Specification		**Manipulated variable**	
Spec	TGAS	Type	Block-Var
Target	850	Block	COMB
Tolerance	0.01	Variable	TEMP
		Units	C
Manipulated variable limits			
Lower	0		
Upper	1000		

Table A-4 *Design specification WAT-REF*

Variable		**Definition**	
STEAM		Mole-Flow Stream=WAT-R Substream=MIXED Component=H2O Units=kmol/hr	
CH4		Mole-Flow Stream=TO-REF Substream=MIXED Component=CH4 Units=kmol/hr	
Specification		**Manipulated variable**	
Spec	STEAM	Type	Stream-Var
Target	1.5*CH4	Stream	WAT-R
Tolerance	0.001	Substream	MIXED
		Variable	MOLE-FLOW
Manipulated variable limits		Units	kmol/hr
Lower	0		
Upper	100		

Table A-5 *Design specification WAT-WGS*

Variable		**Definition**	
H2O		Stream-Var Stream=WAT-WG Substream=MIXED Variable=MOLE-FLOW Units=kmol/hr	
H2OGAS		Mole-Flow Stream=TO-WGS Substream=MIXED Component=H2O Units=kmol/hr	
CO		Mole-Flow Stream=TO-WGS Substream=MIXED Component=CO Units=kmol/hr	
Specification		**Manipulated variable**	
Spec	H2O	Type	Stream-Var
Target	3*(CO-H2OGAS)	Stream	WAT-WG
Tolerance	0.001	Substream	MIXED
		Variable	MOLE-FLOW
Manipulated variable limits		Units	kmol/hr
Lower	0		
Upper	100		

Table A-6 *Design specification BP-RATIO*

Variable		**Definition**	
CO		Mole-Flow Stream=TO-SYNT Substream=MIXED Component=CO Units=kmol/hr	
CO2		Mole-Flow Stream=TO-SYNT Substream=MIXED Component=CO2 Units=kmol/hr	
H2		Mole-Flow Stream=TO-SYNT Substream=MIXED Component=H2 Units=kmol/hr	
Specification		**Manipulated variable**	
Spec	SN	Type	Block-Var
Target	1.80	Block	BYPASS
Tolerance	0.001	Variable	FLOW/FRAC
		Sentence	FLOW/FRAC
Manipulated variable limits		ID1	TO-WGS
Lower	0		
Upper	1		

Table A-7 *Design specification GAS-REC*

Variable		**Definition**	
CO2		Mole-Frac Stream=MIXED Substream=MIXED Component=CO2	
Specification		**Manipulated variable**	
Spec	CO2	Type	Block-Var
Target	0.03	Block	SPLIT-1
Tolerance	0.0001	Variable	FLOW/FRAC
		Sentence	FLOW/FRAC
Manipulated variable limits		ID1	TO-REC
Lower	0		
Upper	1		

Table A-8 *Design specification H2-REC*

Variable		**Definition**	
H2		Mole-Flow Stream=MIX1 Substream=MIXED Component=H2 Units=kmol/hr	
CO2		Mole-Flow Stream=MIX1 Substream=MIXED Component=CO2 Units=kmol/hr	
CO		Mole-Flow Stream=MIX1 Substream=MIXED Component=CO Units=kmol/hr	
Specification		**Manipulated variable**	
Spec	SN	Type	Block-Var
Target	2.05	Block	H2SPLIT
Tolerance	0.0001	Variable	FLOW/FRAC
		Sentence	FLOW/FRAC
Manipulated variable limits		ID1	H2REC
Lower	0		
Upper	1		

Appendix 2

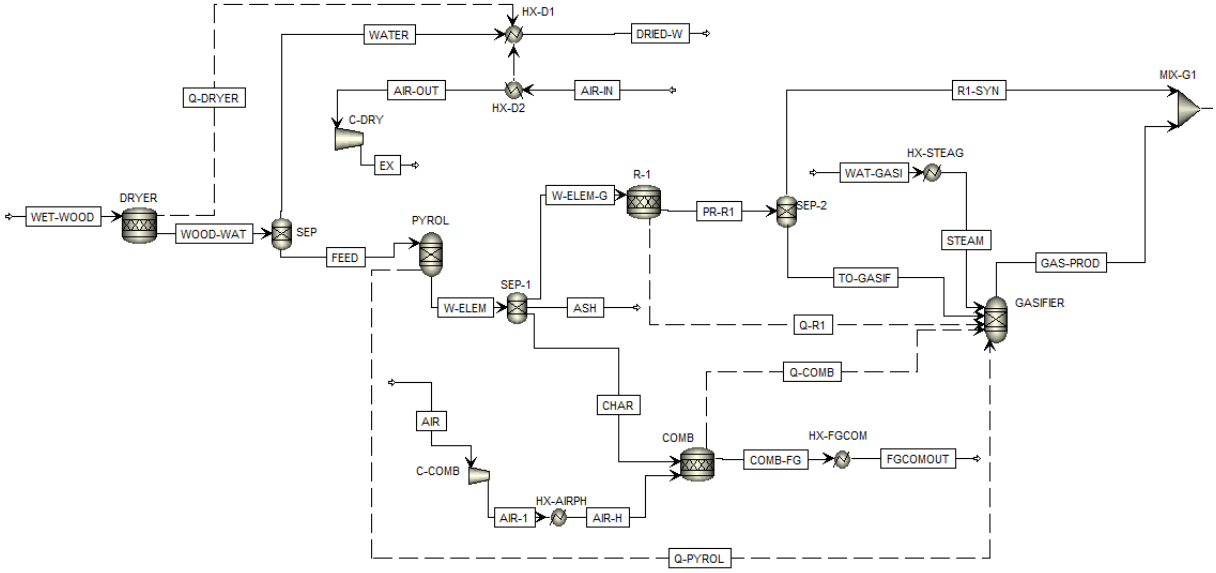

Figure B-1 *Aspen Plus flowsheet simulation of the indirect gasification process*

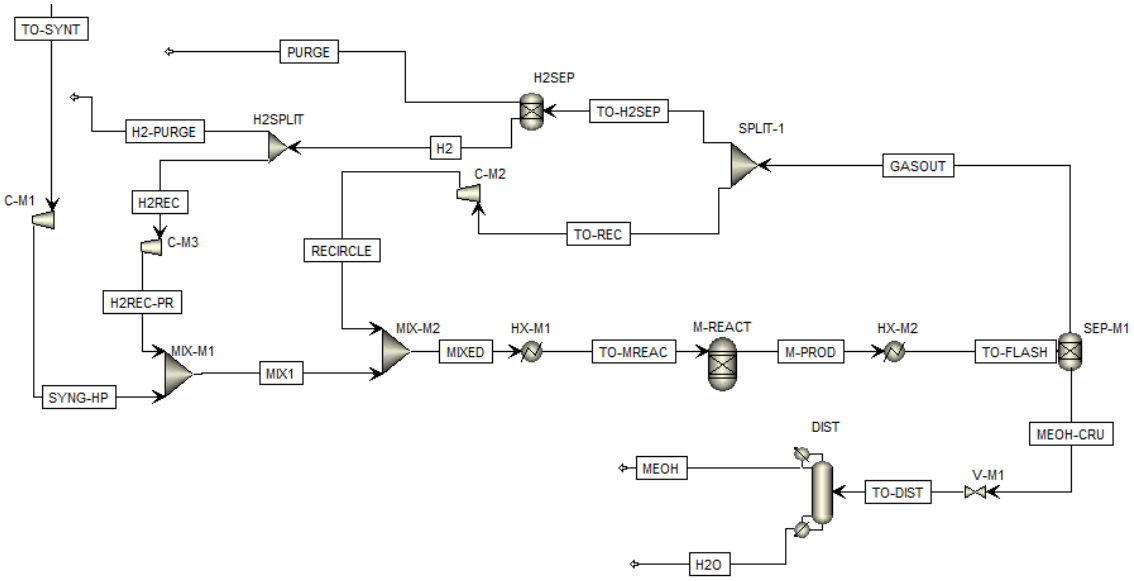

Figure B-2 *Aspen Plus flowsheet simulation of the isothermal low-pressure methanol synthesis, with recirculation of unreacted gas and hydrogen*

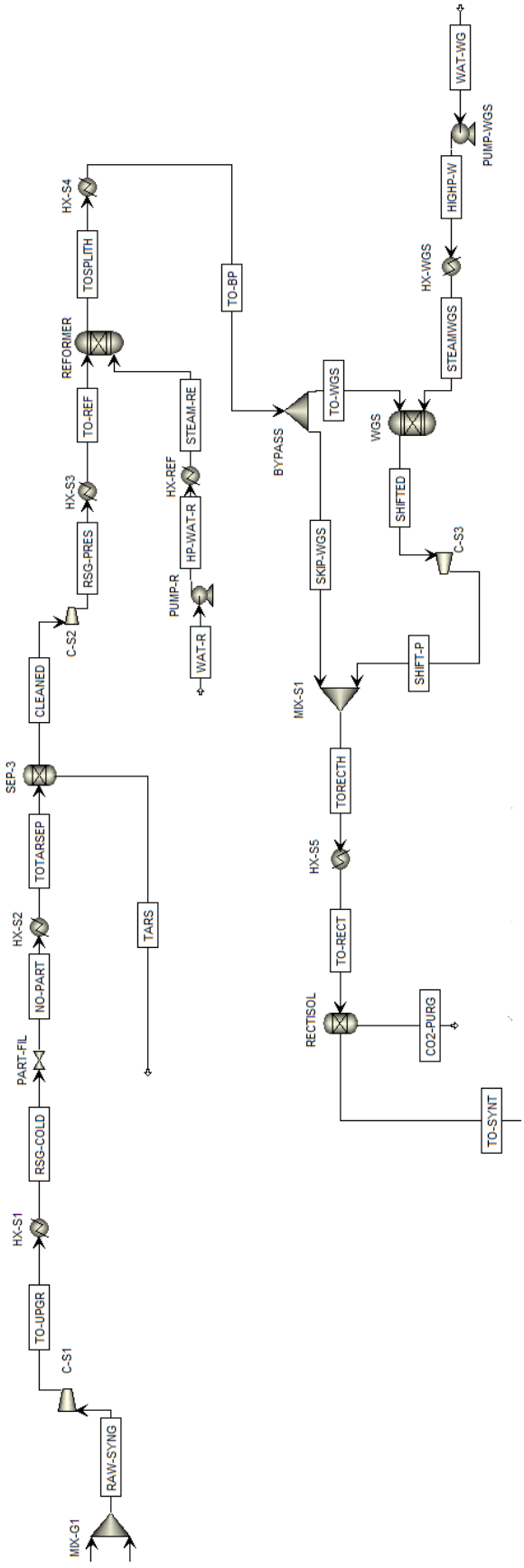

Figure B-3 *Aspen Plus simulation of syngas cleaning and upgrade*

Appendix 3

Table C-1 *Position and production capacity of sawmills in Sweden (only sawmills with production capacity >30,000 m3/year)*

#	Sawmill	Latitude [° N]	Longitude [° E]	Production Capacity [m3/year]
S1	Ala sågverk	61.217476	17.155943	360000
S2	Alvesta sågverk	56.89504	14.53904	130000
S3	Annebergsågen	57.545349	12.176655	100000
S4	AB Högland Såg & Hyvleri	63.308143	18.744582	230000
S5	Sandåsa Timber AB Åkers Sågverk	59.248508	17.116463	100000
S6	Moelven Årjäng Såg AB	59.383498	12.117242	135000
S7	Bergkvist-Insjön AB	60.688862	15.104815	345000
S8	Blyberg Timber Ab	61.150033	14.14319	200000
S9	Bodafors Trä AB	57.576354	14.453591	150000
S10	SCA Wood – Bollsta sågverk	62.993359	17.68226	550000
S11	Vida Borgstena AB	57.886222	13.009149	270000
S12	Holmen Timber AB Braviken Sawmill	58.637702	16.231084	400000
S13	Vida Hjältevad	57.632442	15.360596	200000
S14	Callans Trä AB	62.517422	15.993859	100000
S15	Moelven Dalaträ AB	60.496137	14.967027	144000
S16	Derome Timber AB (Varberg)	57.2344	12.299443	125000
S17	Moelven Edanesågen AB	59.620729	12.815863	120000
S18	Setra Trävaror AB Färila Sågverk	61.804752	15.786832	150000
S19	Fiskarhedens Trävaru AB	61.068617	13.326025	335000
S20	Forssjö Pellets AB	58.948775	16.303437	110000
S21	Gällö Timber AB	62.906889	15.23177	320000
S22	Bergs Timber Gransjö AB	56.739266	15.622413	100000
S23	Stora Enso Timber AB	59.347855	13.12602	320000
S24	Setra Trävaror AB Hasselfors Sågverk	59.092435	14.64818	270000
S25	Vida HN AB	56.289722	13.926064	145000
S26	Setra Trävaror AB Heby Sågverk	59.942879	16.846976	230000
S27	Vida Hestra AB	57.451955	13.588056	170000
S28	AB Hilmer Andersson	59.804187	12.14427	140000
S29	Byggnadssnickerier Krokom AB	63.328562	14.468907	120000

#	Sawmill	Latitude [° N]	Longitude [° E]	Production Capacity [m3/year]
S30	Holmen Timber Iggesunds Sågverk	61.644024	17.093371	340000
S31	Ingarps Lantbruk AB	57.554088	14.985475	100000
S32	Jarl Timber AB	56.687068	15.523269	150000
S33	JGA Sågverket	56.66228	15.136363	175000
S34	AB Karl Hedin Sawmills Karbenning	60.046828	16.078664	220000
S35	Setra Trävaror AB Kastets Sågverk	60.687929	17.257168	230000
S36	Norra Skogsägarna	64.82446	21.03013	220000
S37	Södra Wood Kinda	57.999288	15.657414	220000
S38	Derome Timber AB (Torup)	57.03166	13.10114	115000
S39	AB Karl Hedin Sågverk Krylbo	60.116382	16.215683	250000
S40	Södra Långasjö	56.563697	15.445095	290000
S41	Setra Malå	65.192965	18.717949	175000
S42	Martinsons (HK)	64.363376	20.50655	295000
S43	ATA Timber Moheda AB	57.007895	14.574417	155000
S44	Södra Wood Mönsterås	57.092831	16.538842	420000
S45	Bergs Timber Mörlunda	57.330818	15.883749	110000
S46	SCA Timber AB Munksunds Sågverk	65.281316	21.478903	400000
S47	Moelven Notnäs AB	60.127788	13.013333	190000
S48	Setra Trävaror AB Nyby Sågverk	60.025558	17.54096	190000
S49	Nydala Trävaru AB	57.327361	14.335141	100000
S50	Bergs Timber Orrefors	56.83222	15.783474	125000
S51	Norrskog Wood Products AB	62.424816	15.47213	230000
S52	Rågsveden-Sveden Trä AB	60.701012	13.69588	120000
S53	Rörvik Timber Rörvik AB	57.234512	14.578506	150000
S54	SCA Wood – Rundvik sågverk	63.537375	19.449082	332000
S55	Norra Skogsägarna ek för Sävar Såg	63.911491	20.538089	170000
S56	Siljan Timber AB	60.999369	14.58388	230000
S57	Setra Trävaror AB Skinnskatteberg Sågverk	59.834531	15.690279	250000
S58	Stenvalls Trä AB (Pitea)	65.308762	21.470869	100000
S59	Stenvalls Skogar AB	65.527746	21.178227	180000
S60	SCA WOOD AB Tunadals Sågverk	62.418395	17.385822	500000

#	Sawmill	Latitude [° N]	Longitude [° E]	Production Capacity [m3/year]
S61	Ture Johanssons Trävaru AB	57.351602	14.093014	100000
S62	Södra Wood Unnefors	57.6211	13.766535	110000
S63	Vida Urshult AB	56.525816	14.818083	175000
S64	Moelven Valåsen Wood	59.316218	14.583527	320000
S65	Södra Cell Värö	57.223976	12.175767	590000
S66	Bergs Timber Vimmerby	57.63923	15.871596	130000
S67	Vida Skog AB	56.790283	14.455192	280000
S68	Wallnäs Timber AB	57.616681	15.473717	125000
S69	Älgsjö Såg AB	63.012827	18.212871	30000
S70	Älvsbyn såg	65.679807	20.989649	55000
S71	Åsljunga Pallen AB	56.340306	13.342568	80000
S72	Balungstrands Sågverk AB	60.896491	15.740878	65000
S73	Bäckebrons Sågverk AB	59.663853	13.16379	40000
S74	Bennsäters Sågverk AB	56.504317	15.428061	30000
S75	Bloms Trä Försäljnings AB	57.70849	14.679458	40000
S76	Boda Såg i Dalarna AB	60.719198	15.865632	40000
S77	Brattby Sawmill AB	63.918327	19.879821	70000
S78	Rimbo Timber	59.774659	18.43634	30000
S79	Edsele Såg AB	63.435397	16.532715	30000
S80	Eksjö Industri AB	57.661229	14.984339	60000
S81	ELE Trävaru AB	61.237624	16.561398	35000
S82	ATA Timber Eneryda AB	56.702301	14.35389	60000
S83	Fegens Sågverk AB	57.160025	13.421136	60000
S84	Frödinge Sågverks AB	57.707037	16.01281	45000
S85	Furudals sågverk	61.17095	15.105619	90000
S86	AB Gyllsjö Träindustri	56.193498	13.135269	70000
S87	Hållanders Sågverk AB	57.597377	13.537414	75000
S88	Hjortkvarn Timber AB	58.899955	15.427825	70000
S89	Jutos Timber AB	66.792448	22.924688	65000
S90	Karl Segerström AB	59.965217	15.836098	55000
S91	AB Gustaf Kähr	56.748293	15.917529	50000
S92	AB Krekula & Lauri Såg	67.18926	22.596336	65000
S93	Levene Såg AB	58.325981	12.934783	40000
S94	Liareds Trävaror AB	57.849017	13.716055	35000
S95	Holmen Timber Linghems sågen	58.441706	15.776442	80000
S96	Ljungträ AB	59.532743	16.1263	45000

#	Sawmill	Latitude [° N]	Longitude [° E]	Production Capacity [m3/year]
S97	Lundbergs Trä AB	65.637693	19.139397	35000
S98	Derome Timber AB (Falkenberg)	57.25063	12.810835	40000
S99	Rundvirke Skog AB	61.270182	16.871034	30000
S100	Martinsons Såg (Hallnas)	64.327003	19.533699	75000
S101	Martinsons Såg AB (Kroksjön)	64.703366	20.908015	75000
S102	NK Lundströms Trävaror AB	63.989893	19.726874	60000
S103	Nordanå Trä AB	61.348609	16.036929	65000
S104	Moelven Norsälven AB	59.398168	13.2218	80000
S105	VIDA Nössemark	59.126307	11.820234	95000
S106	AB Okome Träindustri	57.052241	12.695	45000
S107	Södra Wood Orrefors	56.836914	15.745378	70000
S108	Östanåsågen AB	61.365281	15.919837	38000
S109	Moelven Ransbysågen AB	60.674911	12.937627	70000
S110	Setra Rolfs	65.853998	23.115622	80000
S111	Rödins Trävaru AB	62.794751	14.47557	60000
S112	Rydaholms Träförädling AB	56.9909	14.308513	30000
S113	AB Karl Hedin Sågverk	60.34475	15.740816	50000
S114	Stenvalls Trä AB (Lulea)	65.713926	22.262745	80000
S115	Södra Wood Torsås	56.407754	16.000327	85000
S116	ATA Timber Widtsköfle AB	55.859971	14.085838	75000

Appendix 4

Table D-1 *Location of Swedish ports and loaded cargo for international and domestic shipping in 2016 [71]*

Port	Latitude [° N]	Longitude [° E]	Loaded cargo [kt]	
			International	Domestic
Delta Terminal	62.507255	17.49362	22	19
Gävle	60.694005	17.21486	1409	69
Göteborg	57.698217	11.90331	17325	1779
Hallands hamnar	57.116371	12.24588	1755	38
Hargshamn	60.170045	18.47591	72	38
Helsingborg	56.019918	12.70763	3114	569
Husum	63.317733	19.16394	539	159
Kalmar	56.657271	16.37154	280	82
Karlshamn	56.163252	14.83819	1757	75
Karlskrona	56.159009	15.58592	986	0
Landskrona	55.861796	12.83352	150	8
Luleå	65.606066	22.14747	2916	1197
Lysekil	58.275961	11.45368	27	5
Malmö	55.620729	13.03805	3165	50
Mälarhamnar	59.59064	16.51844	313	97
Mönsterås	56.966677	16.44149	468	17
Norrköping	58.619985	16.23228	1405	61
Oskarshamn	57.258253	16.48105	261	208
Oxelösund	58.668544	17.1224	1389	141
Piteå	65.247167	21.625416	808	86
Skellefteå	64.680701	21.23777	695	107
Stockholm	59.335613	18.13269	2673	278
Sundsvall	62.407541	17.38338	1106	36
Söderhamn	61.213583	17.15326	507	6
Södertälje	59.16705	17.65843	27	69
Sölvesborg	56.03465	14.57617	66	0
Trelleborg	55.37245	13.14982	5528	2
Uddevalla	58.350602	11.91547	524	5
Umeå	63.698829	20.3516	1163	3
Vänerhamn	59.317553	14.09379	608	70
Västervik	57.755722	16.64896	0	14
Wallhamn	58.011411	11.69349	241	0
Ystad	55.427104	13.83219	1732	8
Åhus	55.929324	14.32049	140	1

Port	Latitude [° N]	Longitude [° E]	Loaded cargo [kt]	
			International	Domestic
Örnsköldsvik	63.284467	18.73426	390	25
Gotland[1]	57.633844	18.279846	18	460

[1] not included in the model

Appendix 5

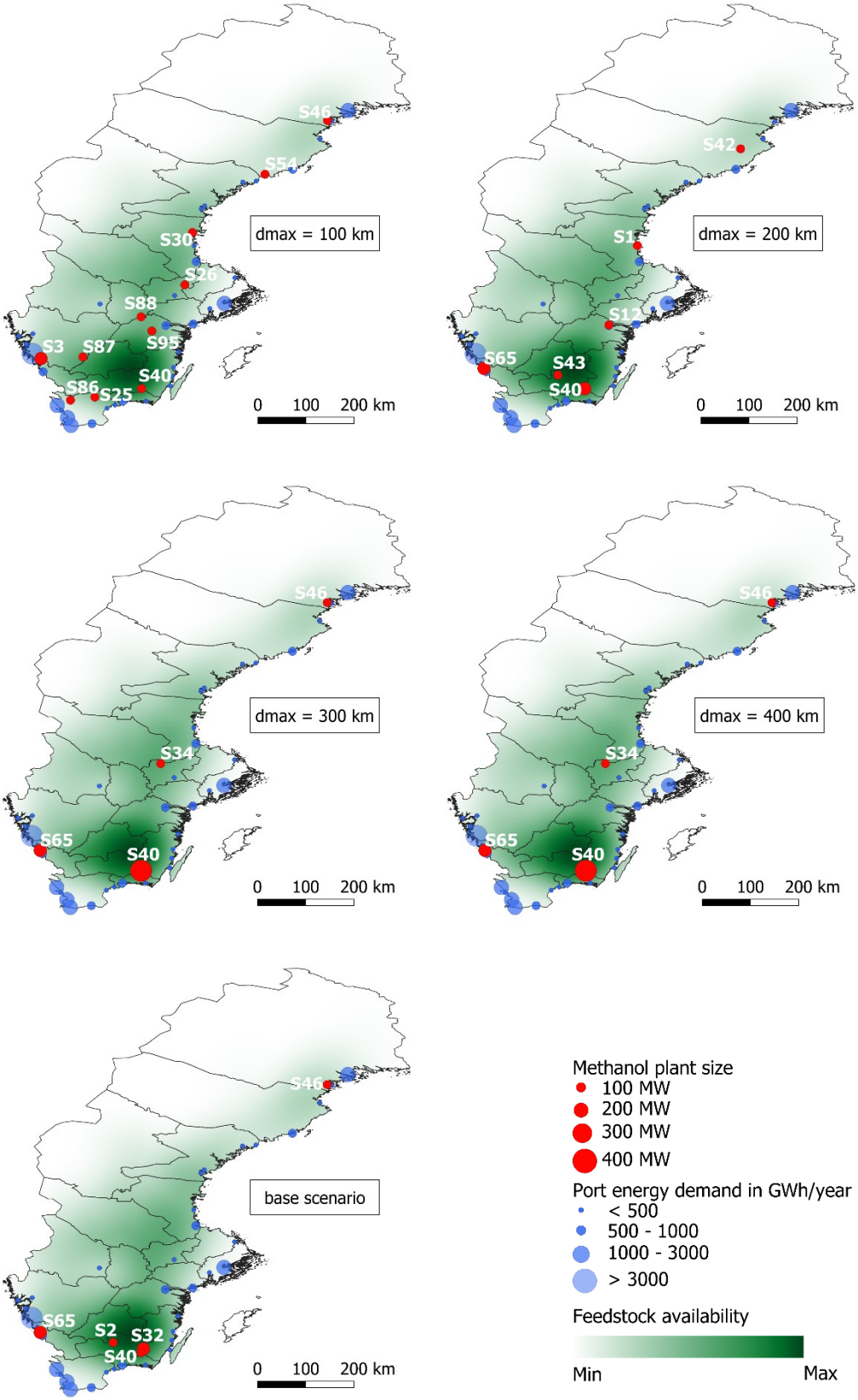

Figure E-1 *Bio-methanol plants individuated for different maximum methanol delivery distance imposed in M5 scenario*

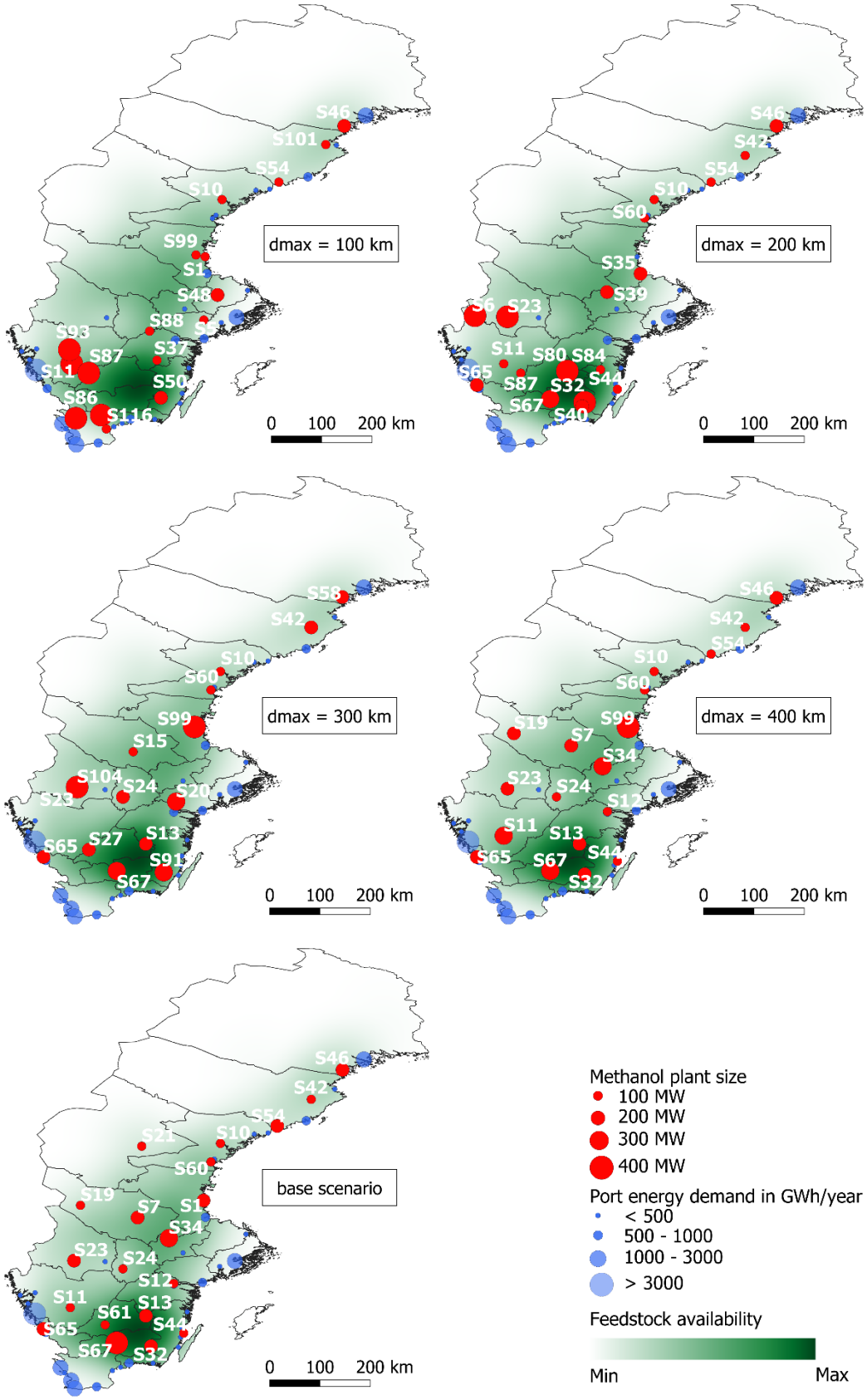

Figure E-2 *Bio-methanol plants individuated for different maximum methanol delivery distance imposed in M25 scenario*

Appendix 6

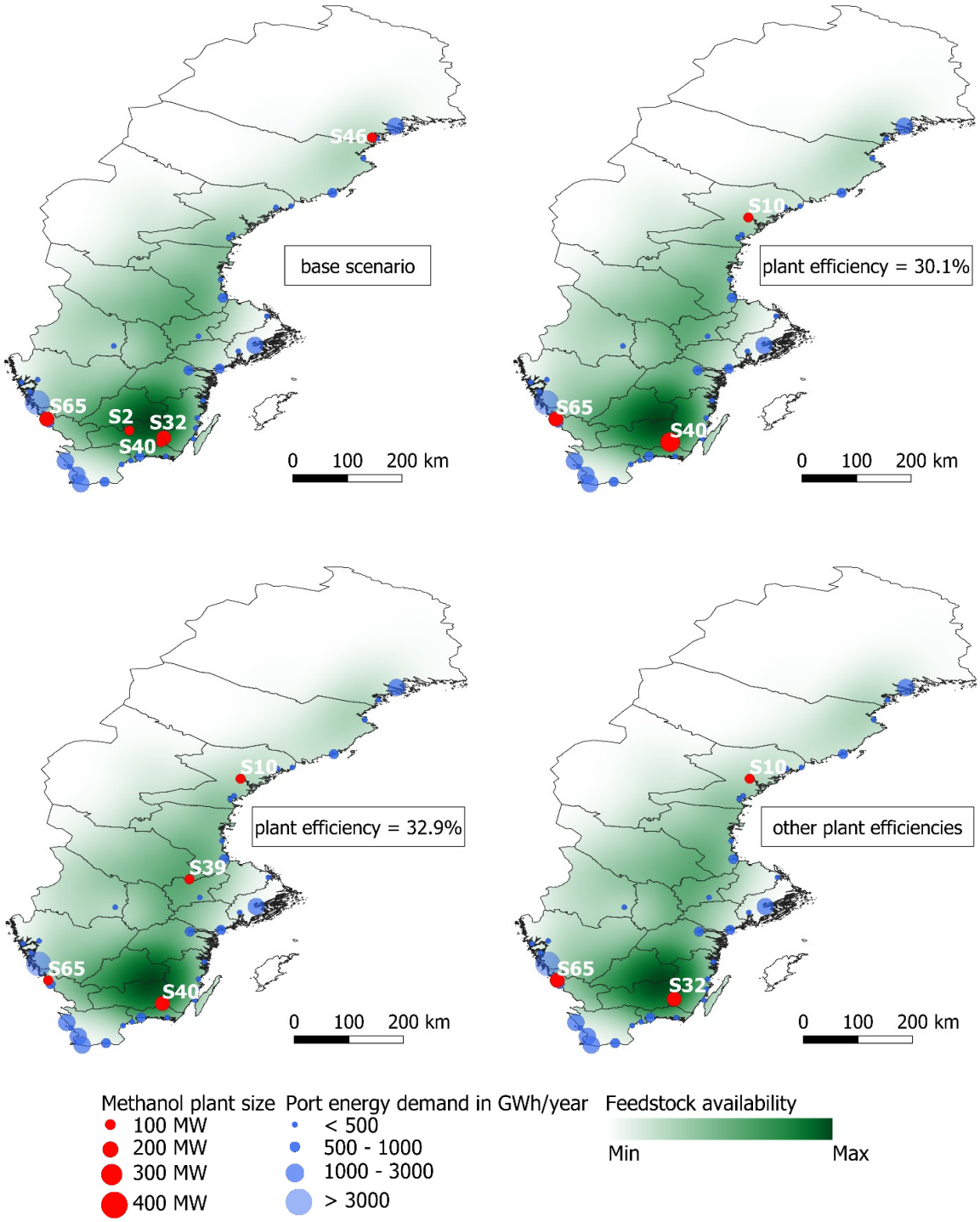

Figure F-1 *Bio-methanol plants individuated in M5 scenario for different assumed plant conversion efficiencies*

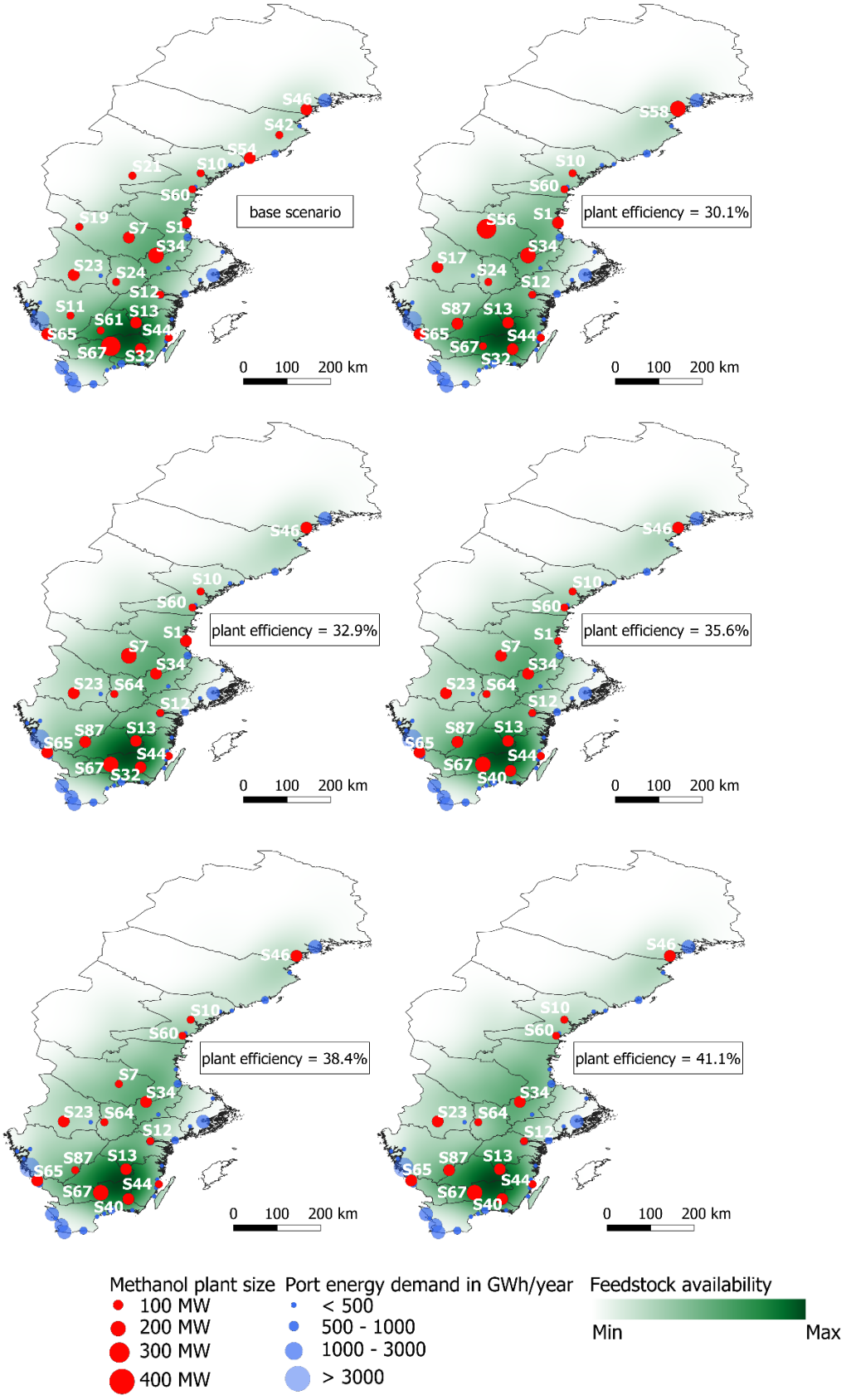

Figure F-2 *Bio-methanol plants individuated in M25 scenario for different assumed plant conversion efficiencies*